

# NASA Technical Memorandum 87671

NASA-TM-87671 19860015201

## Loads and Motions of an F-106B Flying Through Thunderstorms

Roger M. Winebarger

MAY 1986



NASA Technical Memorandum 87671

# Loads and Motions of an F-106B Flying Through Thunderstorms

Roger M. Winebarger  
*Langley Research Center*  
*Hampton, Virginia*

**NASA**  
National Aeronautics  
and Space Administration  
**Scientific and Technical  
Information Branch**

1986

## SUMMARY

Data are presented on loads and motions of a NASA F-106B airplane flying inside thunderstorms; the data cover operations in areas of thunderstorms that produced air-borne weather radar return between 29 and 50 dBZ within 200 miles of the Langley Research Center.

Three pilots were involved; no significant differences in piloting techniques were observed. The thunderstorm flight data were compared with data from other thunderstorm missions and from three airline transport airplanes over their total passenger-carrying operational spectrum from takeoff to landing. The data comparisons indicate that airliners in normal operations occasionally encounter turbulence almost as severe as that encountered in these thunderstorm flights. The maximum derived gust velocity  $U_{de}$  of  $\pm 45$  ft/sec measured in this program was about two thirds of the 65 ft/sec measured in a Thunderstorm Project conducted in the early to mid-1950's. The lower  $U_{de}$  experienced may be a result of the restriction in thunderstorm intensity imposed in this project.

## INTRODUCTION

The National Aeronautics and Space Administration has been conducting a study of the hazards involved in operating aircraft in severe storms. Data are being obtained by flying a highly instrumented F-106B airplane through thunderstorms within 200 miles of the Langley Research Center, Hampton, Virginia, as described in references 1, 2, and 3. Current emphasis is on lightning hazard characterization, and over 600 direct strikes to the airplane have been experienced. In addition, the airplane loads, motions, and control inputs experienced in the thunderstorm environment have been examined and are given in this report. These data have been compared with results from 1941 through 1947 "Thunderstorm Project" (ref. 4), the "Rough Rider" project (ref. 5), and NACA/NASA "VGH" and "Digital VGH" programs taken during normal operations of commercial air transports (refs. 6 and 7). Although in normal transport operations, thunderstorms are avoided when possible, sometimes they are unavoidable and in other instances the airplane is inadvertently flown into a thunderstorm. Therefore knowledge of that environment is needed. Methods of analyzing gust loading of airplanes used herein are presented in references 7 through 10.

## SYMBOLS

$a_n$	incremental normal acceleration from steady-state lg unaccelerated flight, g units
$c$	mean wing chord, ft
dBZ	logarithmic scale of radar measure of water content
$g$	acceleration due to gravity, $32.2 \text{ ft/sec}^2$

$K_g$	gust factor, $\frac{0.88\mu_g}{5.3 + \mu_g}$
$k_o$	reduced frequency parameter for zero crossings
$m$	lift-curve slope, per radian
$N_o$	number of zero crossings per unit time with positive slope
$S$	wing area, $\text{ft}^2$
$U_{de}$	derived gust velocity, $\frac{2a_n W}{m\rho_o S V_e K_g}$ , ft/sec
$V$	true airspeed, ft/sec
$V_e$	equivalent airspeed, $V\sqrt{\frac{\rho}{\rho_o}}$ , ft/sec
$W$	airplane weight, lb
$\mu_g$	airplane mass ratio, $\frac{2W}{m\rho_o c g S}$
$\rho$	atmospheric density, slugs/ $\text{ft}^3$
$\rho_o$	atmospheric density at sea level, slugs/ $\text{ft}^3$

#### TEST EQUIPMENT

##### F-106B Research Airplane

A highly instrumented F-106B "Delta Dart" airplane (fig. 1) is used to make thunderstorm penetrations in the Storm Hazards Program. Details on the F-106B airplane and the criteria used in choosing the airplane for this mission can be found in references 1 and 2. Prior to each thunderstorm season the airplane is prepared to safely take direct lightning strikes (lightning hardened) and the preparation verified by a ground test simulating lightning strikes. The lightning hardening procedures and verification tests are described in references 1 and 3. Although the airplane has undergone extensive modifications to incorporate the instrumentation system, the aerodynamic characteristics remain unchanged. Characteristics of the airplane pertinent to the evaluation of the data are as follows:

Takeoff weight, lb .....	35 000
Typical fuel burn in 90-min flight, lb .....	6000
Wing area, $S$ , $\text{ft}^2$ .....	700
Fin and rudder area, $\text{ft}^2$ .....	105
Wing mean geometric chord, $c$ , ft .....	23.76
Lift-curve slope, $m$ , per radian .....	2.9

##### Airborne Instrumentation Systems

The F-106B is equipped with a number of data systems to measure the environmental and electromagnetic characteristics of thunderstorms during penetrations. The

Aircraft Instrumentation System (AIS) measures and records all the airplane environmental and performance data. Accelerations were sensed by the accelerometers mounted as close to the center of gravity as practical such that the measurement error due to displacement from the center of gravity will be no greater than 2 percent.

### Test Procedures and Data Selection

All the pilots agreed to fly the thunderstorm penetrations at a nominal indicated airspeed of 300 knots. Usually, ATC assigned a fixed altitude and the airplane was maneuvered to adhere to that altitude. Also, some maneuvering was included when a line of several cells was penetrated. The cells usually did not line up in a straight line and sometimes a turn would be initiated before a cell was exited and sometimes the next cell would be entered before the turns were completed. The data used for this paper were truncated at the beginning and end of penetrations to minimize maneuver influences on the data shown. All data shown were taken inside the thunderstorms.

Figure 2 shows the number of penetrations versus penetration duration during the summer 1982 season; 192 thunderstorm penetrations were involved with a total time inside thunderstorms equal to 398.1 min (6.63 hr). The average penetration lasted about 2.07 min. The dates, places, and flight number for each pilot is given in table I. Flights analyzed in this report comprise only 16 percent of the total number of flights in the program through 1984. The airborne weather radar return for the area of the storms that the airplane penetrated was between 29 and 50 dBZ, although the maximum radar reflectivity frequently exceeded the 50 dBZ operating limit. Storm return on the airborne radar was used for guidance into the storm; 29 dBZ was the lowest level the radar would show. Penetrations into areas of the storm with levels in excess of 50 dBZ were avoided to preclude hail encounters. Figure 3 shows the distribution of penetration altitudes which range from 10 000 to 38 000 ft pressure altitude.

The level crossings of various flight parameters were counted when the value crossed the given level with a positive slope for positive levels, and when it crossed the given level with a negative slope for negative levels; zero was considered a positive level (ref. 6). The same level can be counted more than once without the value becoming zero. Also, the maximum positive and negative values were established for each penetration; each curve dealing with maximum positive or negative value therefore represents 384 data points. The derived gust velocity was calculated by using equation (13) from reference 8; that is,

$$U_{de} = \frac{2W a_n}{K_g \rho_o V_e m S}$$

with a constant lift-curve slope of 2.9. Fuel burn was taken into account to establish airplane weight; weight decrease due to fuel burn was about 6000 lb during a typical flight lasting 90 minutes. During storm penetrations, changes in normal acceleration were taken with respect to steady-state lg conditions; altitude changes were taken with respect to the average altitude for that penetration.

## RESULTS AND DISCUSSION

### Data Presentation

The histogram of penetration duration in figure 2 shows that most penetrations had durations from 0.5 to 2.5 min; the longest durations were up to 9 min. Since the data from some penetrations were truncated to eliminate maneuvers, the actual time in the thunderstorm was somewhat higher than shown in this figure. Although not a rule, generally the longer the penetration time the bigger and more intense was the thunderstorm. Duration thus gives a qualitative indication of the distribution of storm intensity. The data in figure 3 indicate that about 68 percent of the total time was spent in the pressure altitude interval from 24 000 to 32 000 ft, with the total range being from 10 000 to 38 000 ft.

In figures 4 through 12, data are presented in four forms for each of the following parameters: normal acceleration, lateral acceleration, longitudinal stick position, pitch attitude, lateral stick position, roll attitude, changes in pressure altitude, indicated airspeed, and derived effective gust velocity. In each figure, the total level crossing results are presented in part (a); the level crossings for each of the three pilots are presented in part (b). The maximum positive and negative values of each parameter in each penetration are presented as a percentage basis for all data in part (c) and for each pilot in part (d).

Normal acceleration data are shown in figure 4. A straight line faired through the level crossing rates in figure 4(a) will intercept the  $a_n = 0$  line at about 3000 counts/hr or  $N_O \approx 0.83$  upward crossing/sec. The equations needed to calculate  $N_O$  by means of the methods of the theory of reference 9 are

$$N_O = \frac{Vk_O}{\pi C}$$

where

$$k_O = f(\mu)$$

was obtained from figure 9 of reference 9 and

$$\mu = \mu_g = \frac{2W}{m\rho c g S}$$

Using these equations for the average case of 28 000-ft altitude and 32 000-lb aircraft weight gives  $\mu$  equal to 39.02, and from figure 9 of reference 9,  $k_O$  is equal to 0.084. The penetration velocity at an altitude of 28 000 ft was 760 ft/sec which will yield  $N_O = 0.855$  upward crossing/sec or 3079 counts/hr which agrees well with the approximately 3000 counts/hr indicated in figure 4(a). For the conditions of these flights, that is, flight inside storms with a radar reflectivity of no greater than 50 dBZ, the largest excursion was 1.5g (fig. 4(a)), and for about 90 percent of the penetrations the maximum excursions were less than  $\pm 1g$  (fig. 4(c)). Lateral acceleration data are given in figure 5 with excursions generally being less than  $\pm 0.3g$ . About 90 percent of the penetrations had maximum lateral excursions less than  $\pm 0.2g$  (fig. 5(c)). The normal and lateral acceleration results shown in figures 4(b) and 5(b) show some differences for load increments for

flights flown by the three different pilots. Pilot 1 experienced somewhat higher normal and lateral acceleration increments (figs. 4(b) and 5(b)) than pilot 2, with usually slightly less control input activity (figs. 6(b) and 8(b)). Pilot 3 had only a few flights resulting in a small data sample and considerable scatter in the data points shown for him. These observations and the  $U_{de}$  results shown in figure 12(b) may indicate pilot 1 encountered slightly more severe storms than pilot 2.

Attitude upsets due to storm turbulence and corresponding control inputs to counter the storm effects are indicated by figures 6 through 9. Comparison of data in figures 7(a) and 9(a) show that an attitude excursion of  $10^\circ$  in roll is almost three orders of magnitude more likely to occur than a  $10^\circ$  pitch attitude excursion (relative to the trim pitch attitude of about  $4^\circ$ ). The altitude excursions shown in figure 10 indicate an equal distribution of updrafts and downdrafts. Figure 10(a) shows that excursions of  $\pm 1000$  ft were encountered; figure 10(c) indicates that altitude deviations less than 150 ft were found in about one third of the penetrations. The indicated airspeed variations (fig. 11) reflect primarily the gust component parallel to the direction of flight. These data (fig. 11(b)) show good consistency between the three pilots.

Figure 12(a) shows derived gust velocities  $U_{de}$  up to  $\pm 45$  ft/sec were experienced by the F-106B but over 50 percent of the penetrations resulted in values of  $U_{de}$  less than  $\pm 16$  ft/sec (fig. 12(c)). The curve shown in figure 12(a) for positive  $U_{de}$  represents the faired average curve that is obtained by considering the negative values jointly with the positive values in an absolute value sense. Figure 12(b) shows distributions of  $U_{de}$  for each pilot.

Previous studies (i.e., ref. 9) indicate that an equation of the following type usually fits the storm data of figure 12(a) quite well:

$$N = PN_0 e^{-U_{de}/\sigma_d}$$

where  $P$  is the proportion of time spent in turbulence,  $N_0$  represents upward zero crossings per unit of time, and  $\sigma_d$  is the root-mean-square (rms) value of the turbulence intensity. The data of this report also support this equation. The specific equation representing the faired curve in figure 12(a) is

$$N = 3200 e^{-U_{de}/4.79}$$

Since the flights were virtually all in turbulence,  $P = 1$  in this study, the equations then indicate that  $N_0 = 3200$  counts/hr, or  $N_0 = 0.889$  counts/sec, and  $\sigma_d = 4.79$  fps. This value of  $\sigma_d$  is a derived equivalent gust velocity at sea level. To establish true airspeed values both  $U_{de}$  and  $\sigma_d$  should be multiplied

by  $\sqrt{\frac{\rho_0}{\rho}}$ , where  $\rho_0$  is sea-level density, and  $\rho$  is the density at altitude. An average altitude of 28 000 ft is assumed here; thus,

$$\sqrt{\frac{\rho_0}{\rho}} = 1.576$$

The true rms value is thus found to be  $\sigma_{\text{true}} = 7.55$  fps. This agrees well with the rms values found in previous flight studies through cumulus clouds only, 7.82 ft/sec from figure 2 of reference 10, but is significantly less than the maximum  $\sigma_{\text{true}}$  of 16 ft/sec for flight in severe storms in reference 10 (p. 9). The restriction to dBZ levels below 50 in the present program undoubtedly accounts for the lack of  $U_{de}$  approaching the 16 ft/sec measured in the earlier program.

#### Gust Data Comparisons

Other thunderstorm project results.- In figure 13, the derived gust velocities for the F-106B are compared with the data from reference 4 for the Thunderstorm Project and the thunderstorm data from reference 5 for the Rough Rider project. These data show upward gusts only. The data for the F-106B show general agreement with the previous storm data up to  $U_{de} = 45$  ft/sec, the maximum measured, but the Thunderstorm Project described in reference 4 measured values of  $U_{de}$  approaching 65 ft/sec. The Rough Rider data shown in figure 13 have been extrapolated in reference 5 to higher derived gust velocities than were actually measured.

Air transport results.- The latest  $a_n$  and  $U_{de}$  data from three different air transport airplanes were available from the NASA Digital VGH (DVGH) program and were in the same format, from the same data reduction methods, so that direct comparisons were immediately available. The complete DVGH data set is at present unpublished, although the program is described in references 6 and 7. Over 1600 hours of data were collected for each of the three types of airplanes: Boeing 727, Boeing 747, and Lockheed L-1011. The 727 and 747 flights were in the continental United States and southern Canada with some 747 flights being transatlantic. The L-1011 flights were in the eastern United States and Puerto Rico. Data were taken from 15 sec after takeoff until 15 sec before touchdown. The data were numerically filtered to separate maneuver-induced accelerations and gust-induced accelerations. Although the maneuver-induced accelerations were not numerically filtered from the F-106B data, they were minimized by data selection. The comparison of normal acceleration data is shown in figure 14 and indicates that on the basis of counts per hour the F-106B experienced about  $10^4$  more frequently a gust loading of  $\pm 0.75g$  than did the air transports.

A comparison of the derived gust velocities of the F-106B and the air transports is shown in figure 15. The L-1011 encountered an updraft producing a derived gust velocity almost as large as that encountered by the F-106B (45 ft/sec) but downdrafts of corresponding strengths were not encountered by the L-1011. The 727 encountered downdrafts almost as strong as the F-106B encountered in thunderstorms and updrafts 75 percent as strong. The slope of the L-1011 curve with the updrafts at high  $U_{de}$  values is noted to be about the same as that encountered in the thunderstorm flights. The air transports encounter these highest  $U_{de}$  only a small proportion of the time, but the comparison does show that airliners do occasionally encounter very turbulent conditions of thunderstorm magnitude. The L-1011 high turbulence encounter was in the altitude block 9500 to 14 500 ft, which corresponds to an approach to or departure from the airport where the flexibility to deviate around bad weather decreases. The 727 encounter was in the altitude block 24 000 to 29 500 ft.



## CONCLUDING REMARKS

As part of the NASA Storm Hazards Program, loads, motion, and control input data were obtained for an F-106B airplane flying inside thunderstorms. The storm penetrations were limited to areas of thunderstorms with a radar return of less than 50 dBZ. Penetrations were made over a pressure altitude range of 10 000 ft to 38 000 ft with most of the penetrations around 25 000 ft. The data were presented in terms of the number of times incremental levels were crossed per hour. The data were generally symmetrical about the nominal value. Three different pilots flew the airplane for the storm flights and the piloting techniques were basically the same for all three pilots. Measured normal acceleration zero crossing rate agrees very well with theoretical methods. The maximum derived gust velocity  $U_{de}$  of  $\pm 45$  ft/sec measured in this program was about two thirds of the 65 ft/sec measured in the Thunderstorm Project.

The F-106B response to thunderstorms was found to be far more pronounced in the roll axis than in pitch. As shown by these data a roll attitude excursion of  $10^\circ$  is almost three orders of magnitude more likely to occur than a  $10^\circ$  pitch attitude excursion.

The data were compared with recent airliner data. The comparison showed the L-1011 and the 727 had occasionally encountered updrafts or downdrafts of strengths almost equal to those encountered by the F-106B ( $\pm 45$  ft/sec) in areas of thunderstorms having radar returns less than 50 dBZ.

NASA Langley Research Center  
Hampton, VA 23665-5225  
March 18, 1986

## REFERENCES

1. Fisher, Bruce D.; Keyser, Gerald L., Jr.; Deal, Perry L.; Thomas, Mitchel E.; and Pitts, Felix L.: Storm Hazards '79 - F-106B Operations Summary. NASA TM-81779, 1980.
2. Fisher, Bruce D.; Keyser, Gerald L., Jr.; and Deal, Perry L.: Lightning Attachment Patterns and Flight Conditions for Storm Hazards '80. NASA TP-2087, 1982.
3. Deal, Perry L.; Keyser, Gerald L.; Fisher, Bruce D.; and Crabill, Norman L.: Thunderstorm Hazards Flight Research - Program Overview. AIAA-81-2412, Nov. 1981.
4. Tolefson, H. B.: Summary of Derived Gust Velocities Obtained From Measurements Within Thunderstorms. NACA Rep. 1285, 1956. (Supersedes NACA TN 3538.)
5. Lee, J. T.; and Carpenter, D.: 1973-1977 Rough Rider Turbulence-Radar Intensity Study. Rep. No. FAA-RD-78-115, Mar. 1979. (Available from DTIC as AD A072 693.)
6. Morris, Garland J.; and Crabill, Norman L.: Air Transport Flight Parameter Measurements Program - Concepts and Benefits. SAE Paper 801132, Oct. 1980.
7. Crabill, Norman L.; and Morris, Garland J.: The NASA Digital VGH Program - Early Results. 1980 Aircraft Safety and Operating Problems, Joseph W. Stickle, compiler, NASA CP-2170, Pt. 2, 1981, pp. 613-624.
8. Pratt, Kermit G.; and Walker, Walter G.: A Revised Gust-Load Formula and a Re-Evaluation of V-G Data Taken on Civil Transport Airplanes From 1933 to 1950. NACA Rep. 1206, 1954. (Supersedes NACA TN's 2964 by Kermit G. Pratt and 3041 by Walter G. Walker.)
9. Houbolt, John C.; and Williamson, Guy G.: Spectral Gust Response for an Airplane With Vertical Motion and Pitch. AFFDL-TR-75-121, U.S. Air Force, Oct. 1975. (Available from DTIC as AD A021 713.)
10. Houbolt, John C.; Steiner, Roy; and Pratt, Kermit G.: Dynamic Response of Airplanes to Atmospheric Turbulence Including Flight Data on Input and Response. NASA TR R-199, 1964.

TABLE I.- FLIGHT CREW AND LOCATION FOR DATA FLIGHTS

Flight no.	Date	Pilot	Observer	Location
82-010	5-23-82	W. Neely	P. Deal	Blackstone, Va.
82-013	5-28-82	W. Neely	B. Fisher	Annapolis, Md.
82-017	6-5-82	P. Brown	R. Winebarger	Oregon Inlet, N.C.
82-020	6-27-82	P. Brown	R. Winebarger	Moyock, N.C.
82-021	6-21-82	W. Neely	R. Winebarger	Cape Hatteras, N.C.
82-023	6-29-82	P. Brown	B. Fisher	Nags Head, N.C.
82-024	7-4-82	P. Brown	R. Winebarger	Lynchburg, Va.
82-027	7-11-82	P. Brown	R. Winebarger	Blackstone, Va.
82-028	7-11-82	P. Brown	R. Winebarger	Appomattox, Va.
82-029	7-16-82	P. Deal	R. Winebarger	Salisbury, Md.
82-030	7-17-82	W. Neely	B. Fisher	Chesapeake, Va.
82-032	7-28-82	W. Neely	B. Fisher	Cape May, N.J.
82-033	7-28-82	W. Neely	B. Fisher	Tangier, Va.
82-034	7-30-82	P. Deal	R. Winebarger	Easton, Md.
82-035	7-31-82	P. Deal	B. Fisher	Oceana, Va.
82-037	8-6-82	W. Neely	R. Winebarger	Smith Point, Va.
82-038	8-6-82	W. Neely	B. Fisher	Currituck Sound, N.C.
82-039	8-9-82	W. Neely	R. Winebarger	West Point, Va.
82-040	8-9-82	W. Neely	R. Winebarger	Lawrenceville, Va., to Franklin, Va.
82-041	8-11-82	P. Brown	R. Winebarger	Hopewell, Va.
82-042	8-11-82	W. Neely	R. Winebarger	Scotland Neck, N.C.
82-043	8-17-82	P. Deal	R. Winebarger	Waverly, Va.
82-044	8-25-82	W. Neely	R. Winebarger	Warning Area 72A
82-047	9-20-82	W. Neely	R. Winebarger	Warning Area 72A
82-048	9-20-82	W. Neely	R. Winebarger	Rocky Mount, N.C., to Elizabeth City, N.C.

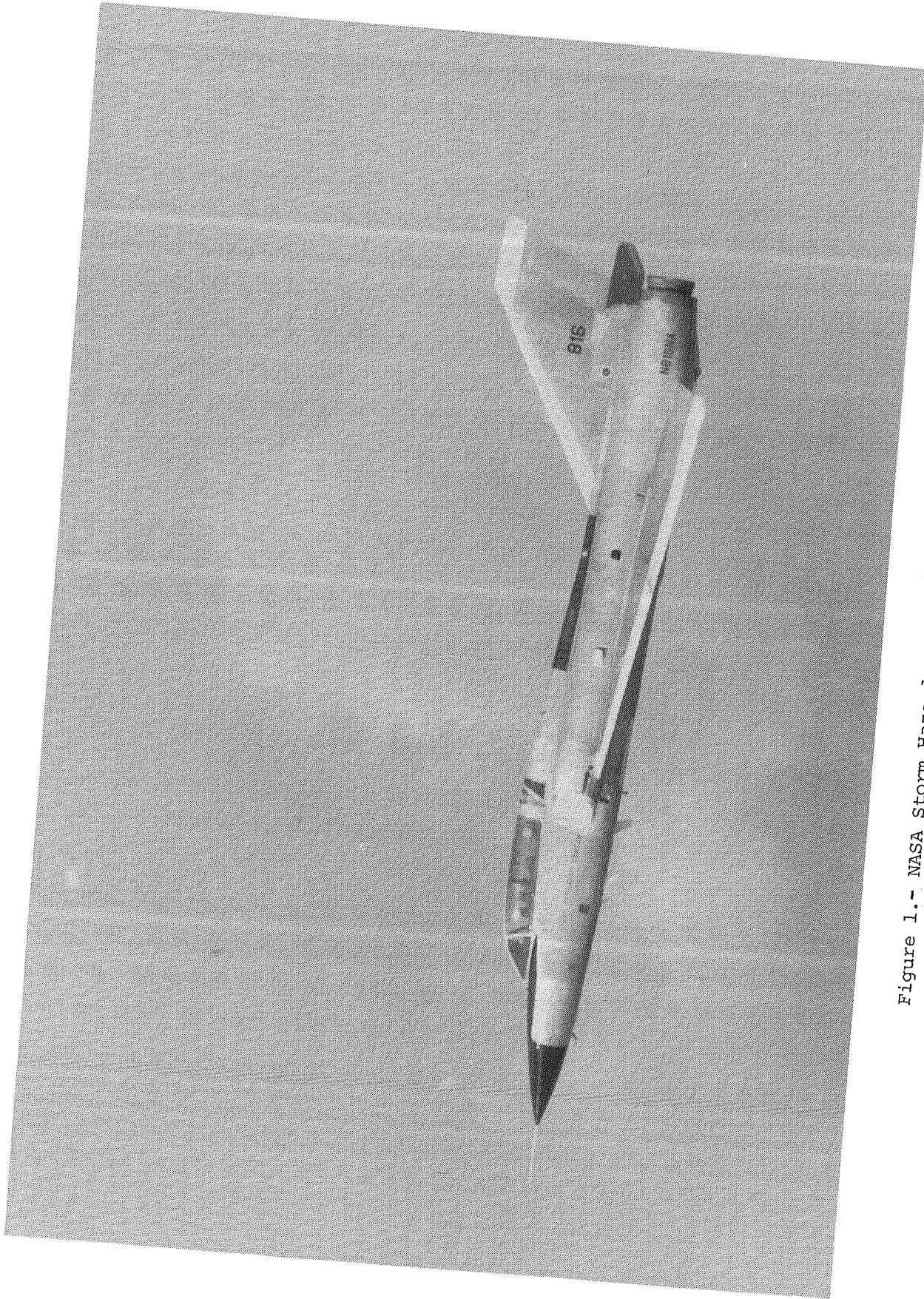


Figure 1.- NASA Storm Hazards Program F-106B airplane.

L-83-2753

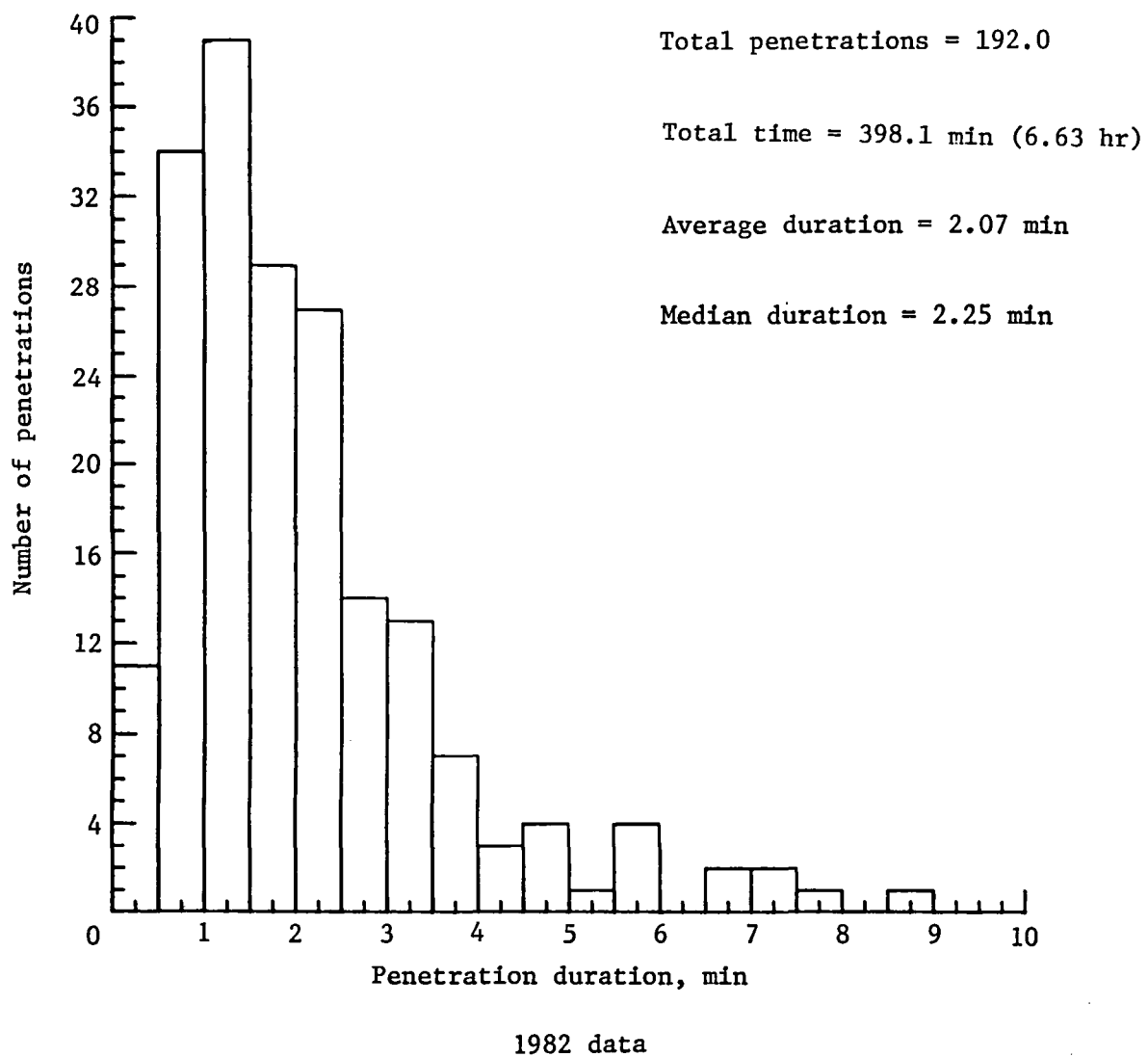


Figure 2.- Distribution of penetration duration.

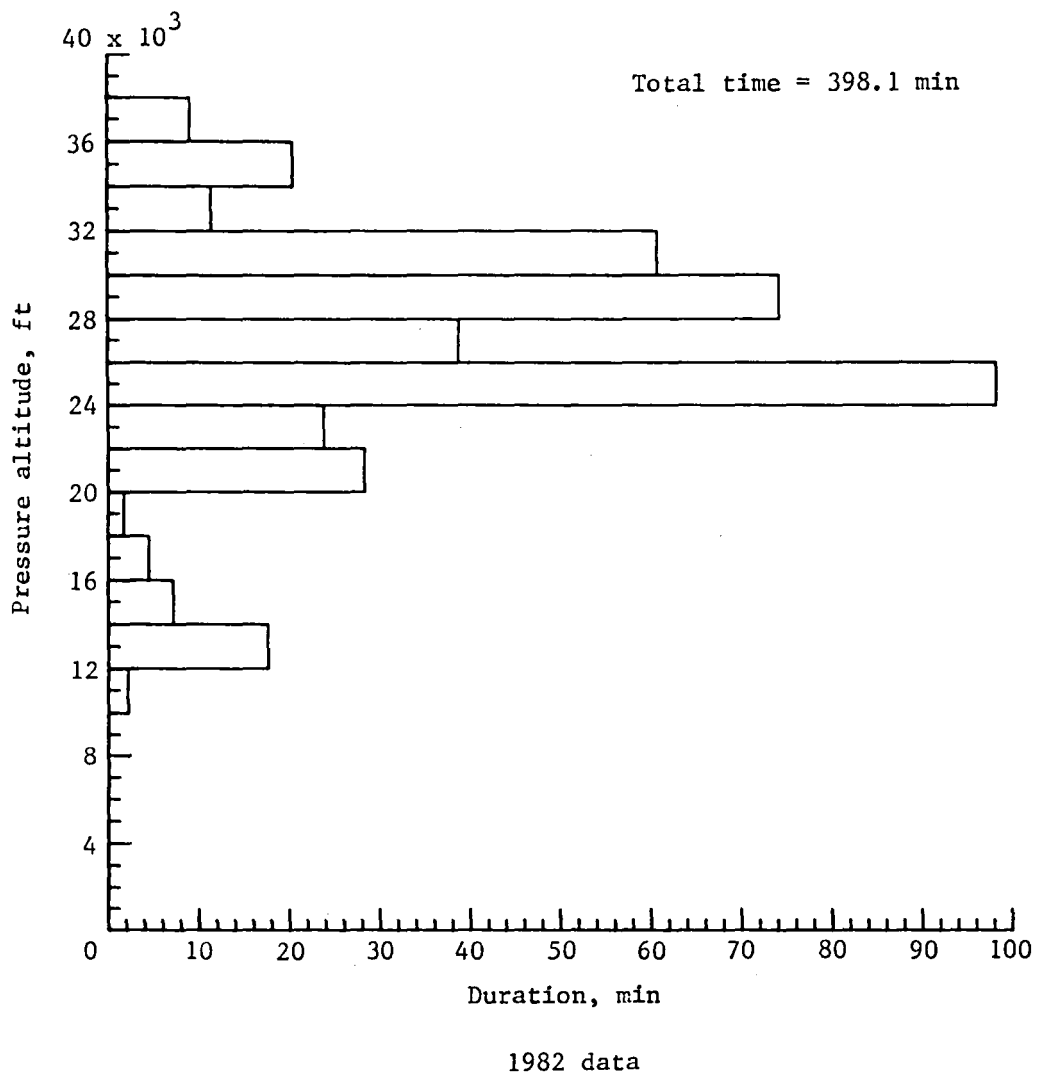
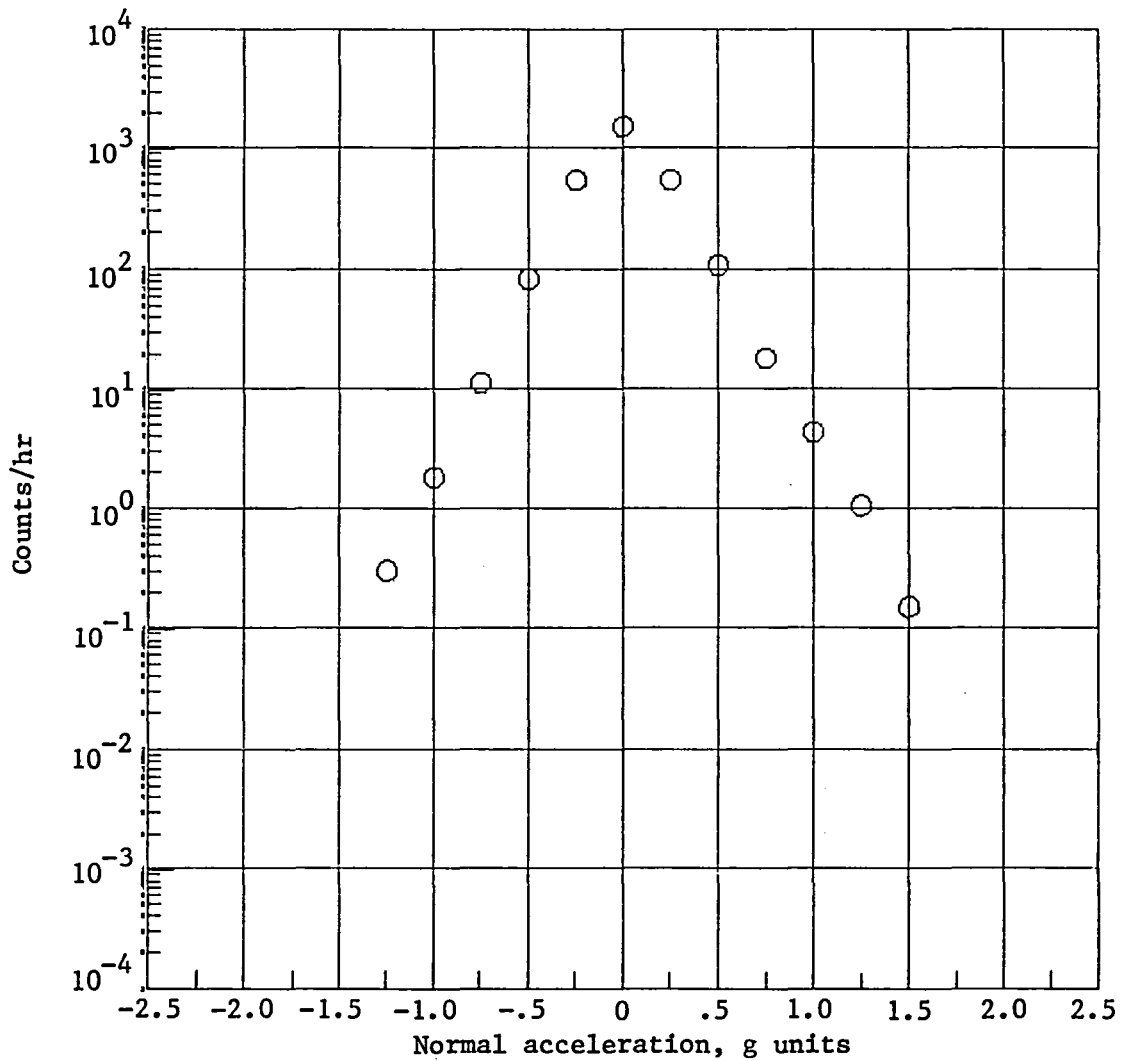


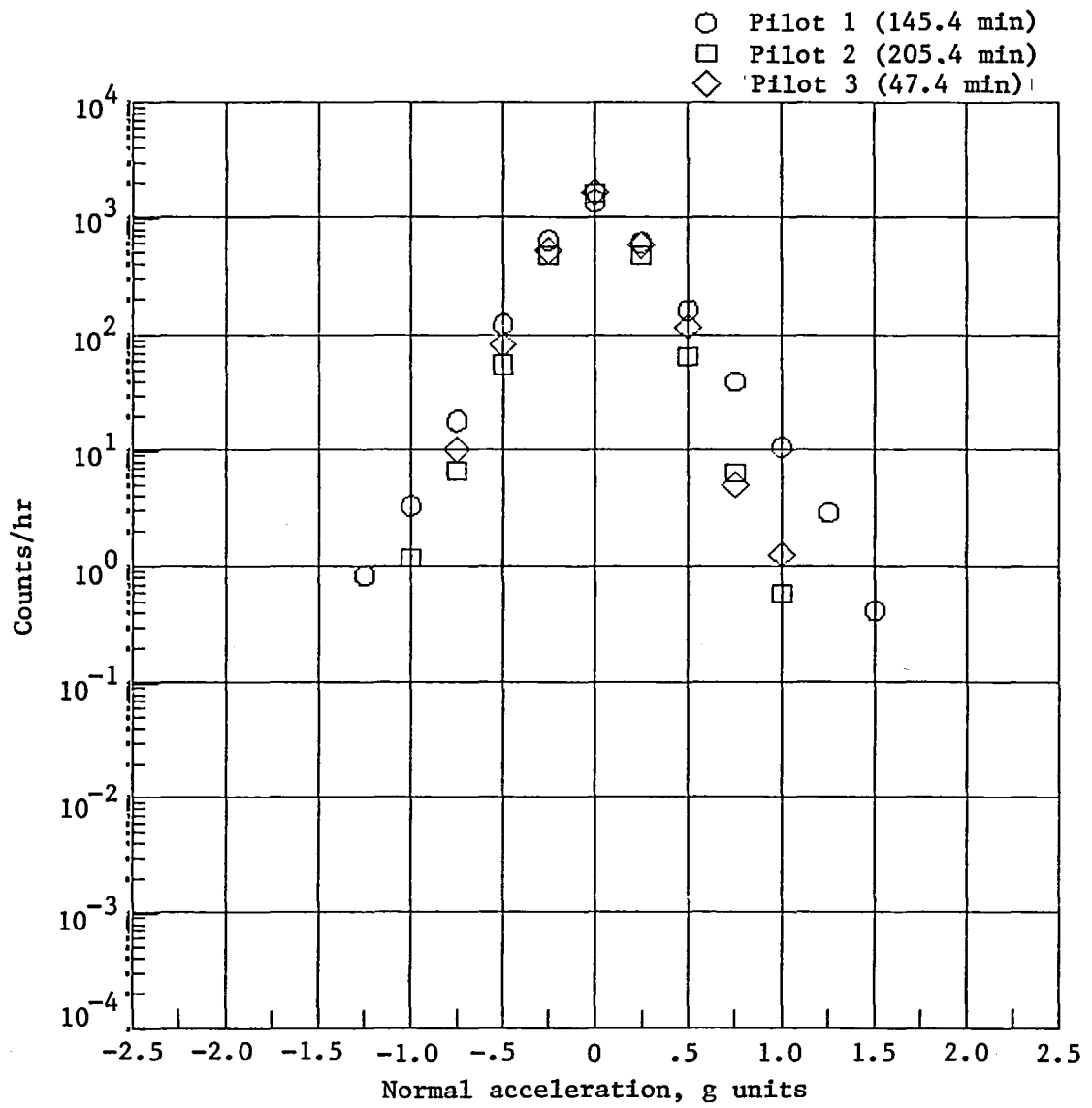
Figure 3.- Distribution of time at altitude.

All pilots (398.1 min)



(a) Level crossing rates for all data.

Figure 4.- Normal accelerations experienced by the F-106B while flying inside thunderstorms.

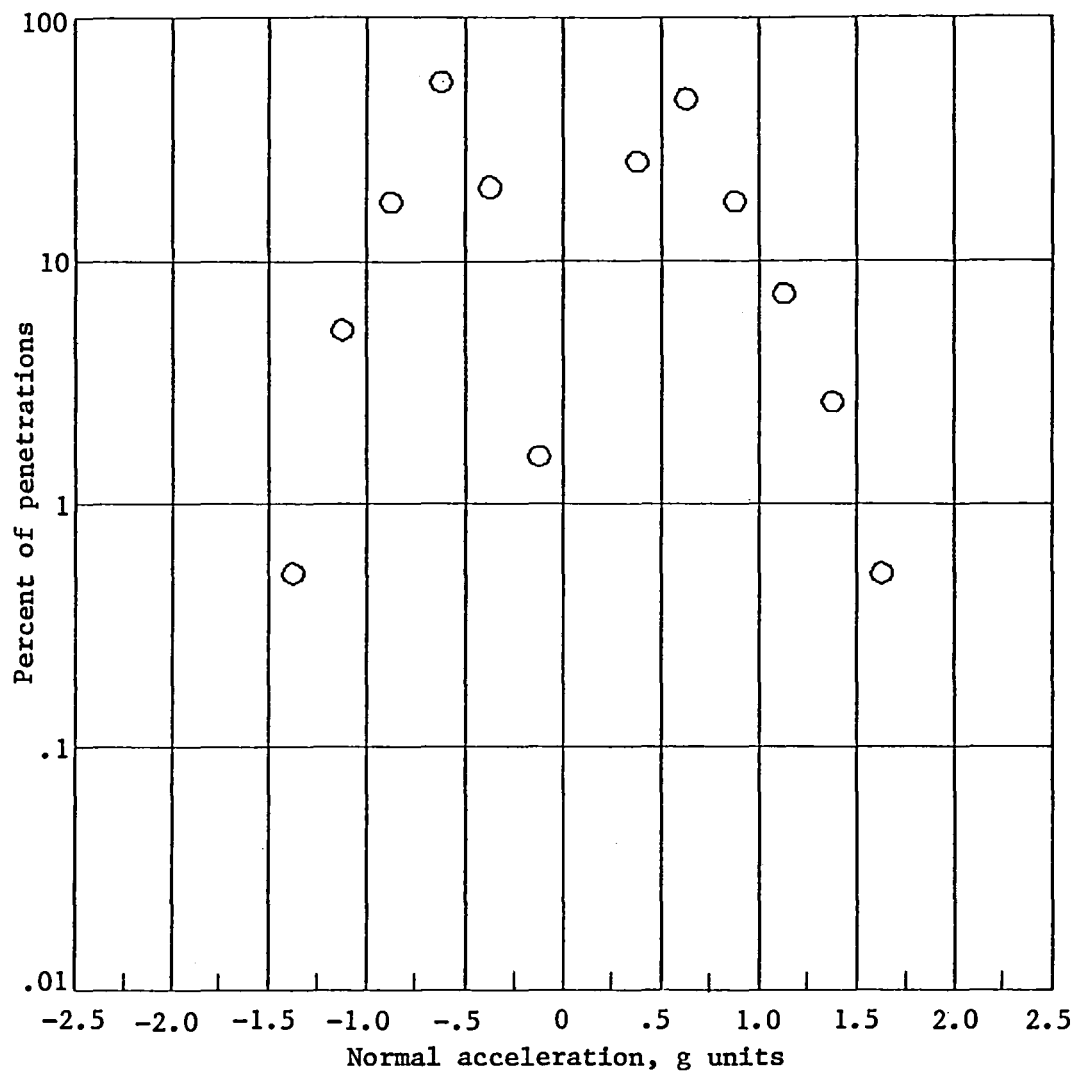


(b) Level crossing rates for each pilot.

Figure 4.- Continued.

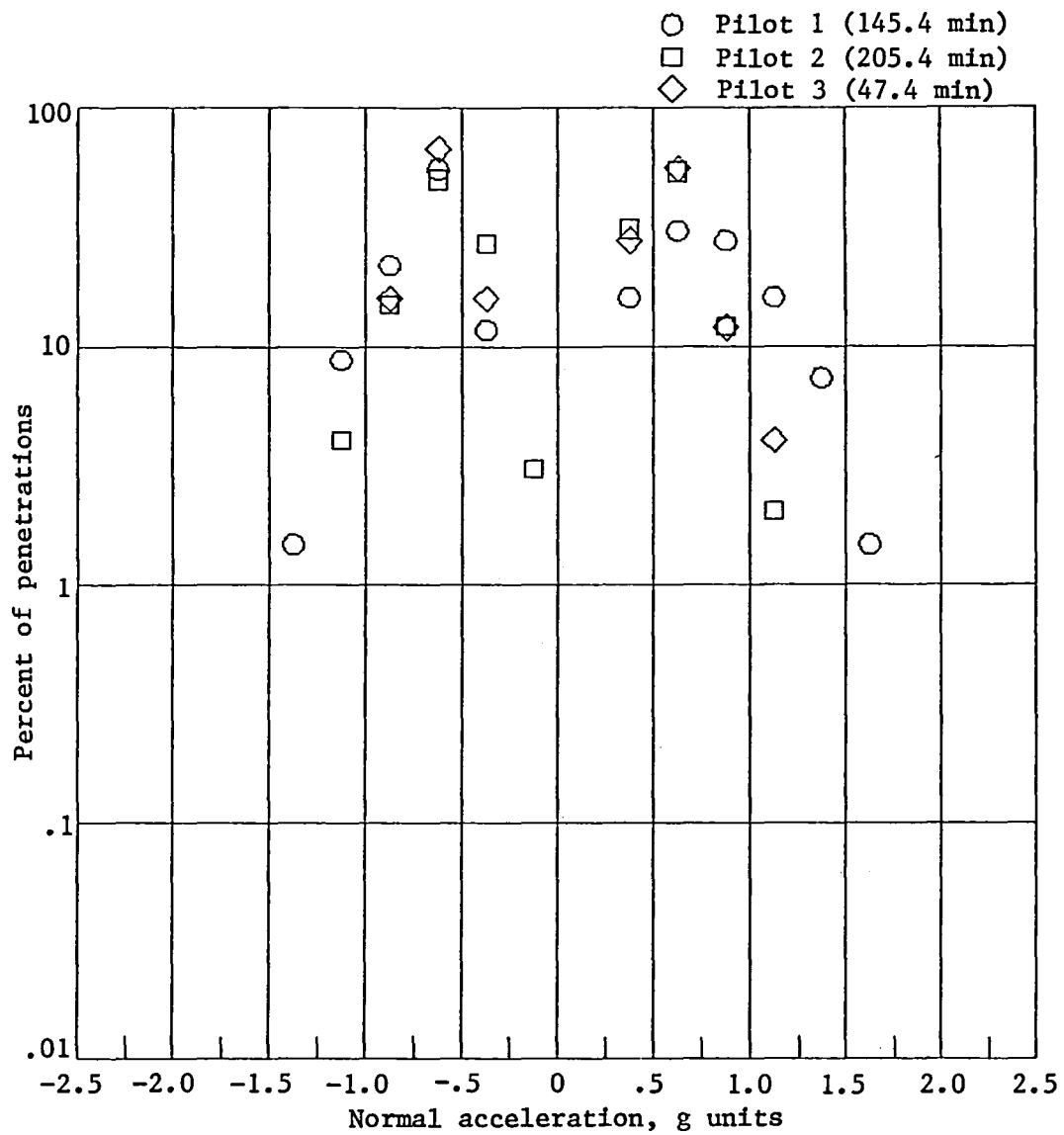


All pilots (398.1 min)



(c) Peak positive and negative occurrences per storm penetration for all data.

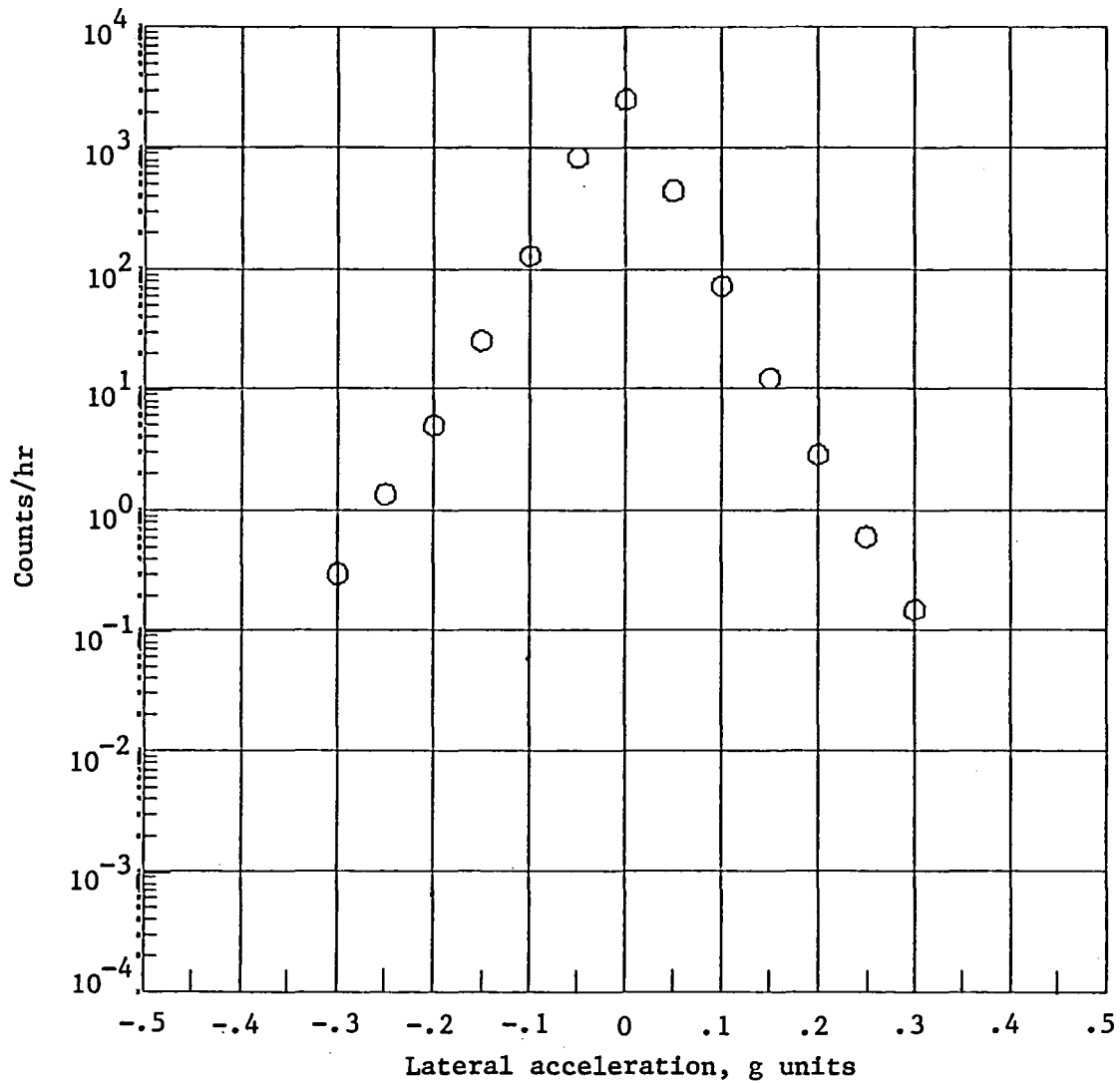
Figure 4.- Continued.



(d) Peak positive and negative occurrences per storm penetration for each pilot.

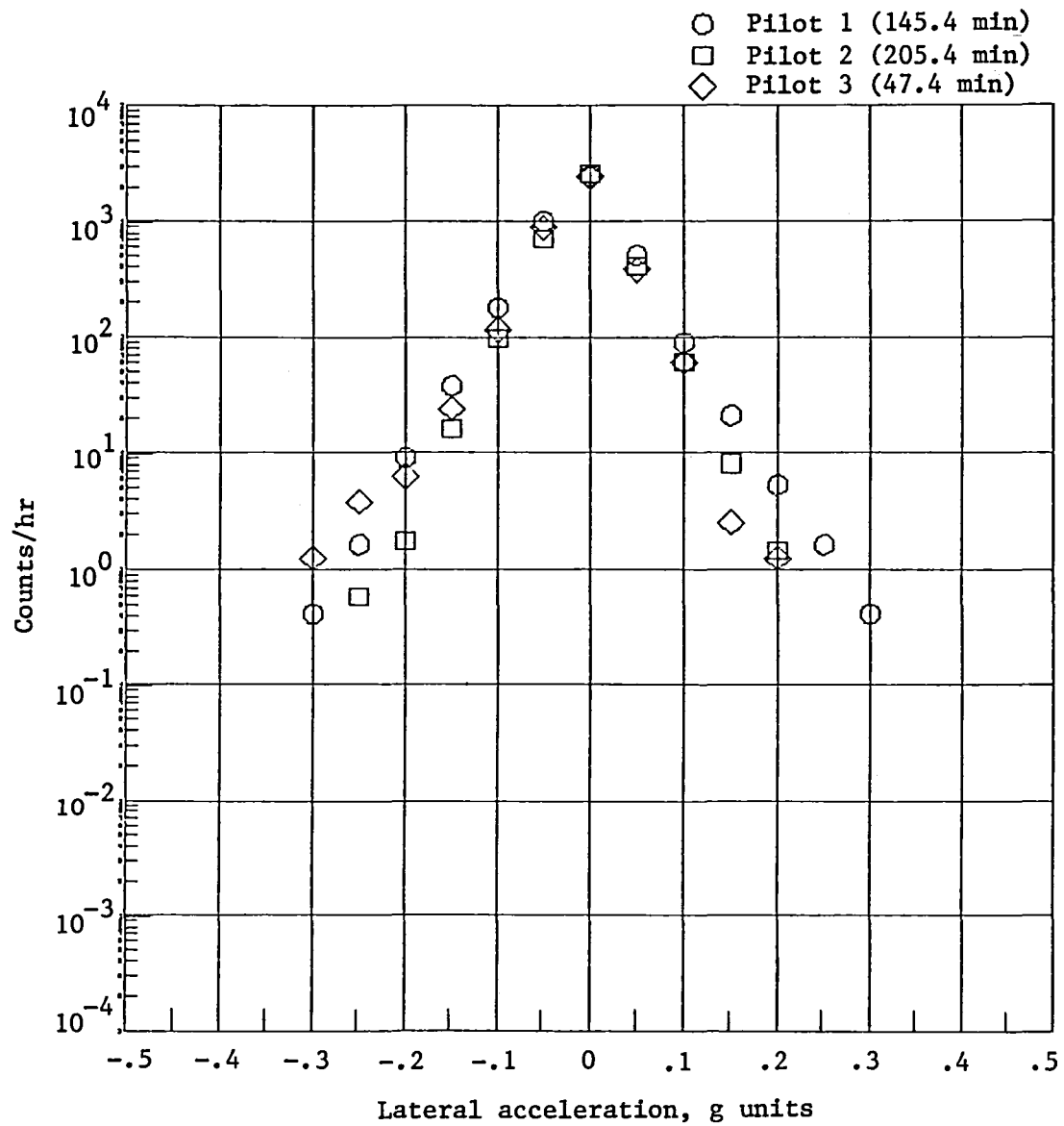
Figure 4.- Concluded.

All pilots (398.1 min)



(a) Level crossing rates for all data.

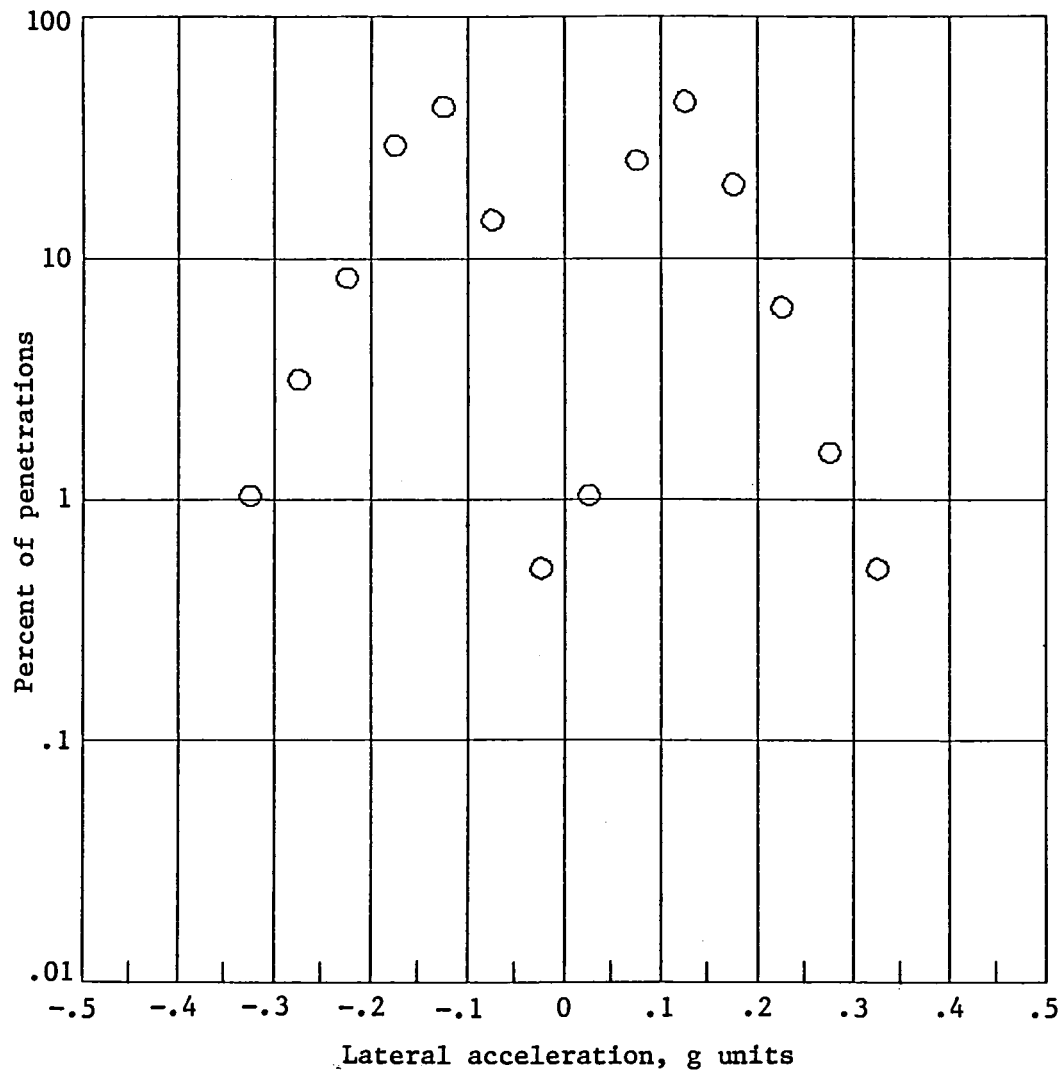
Figure 5.- Lateral accelerations experienced by the F-106B while flying inside thunderstorms.



(b) Level crossing rates for each pilot.

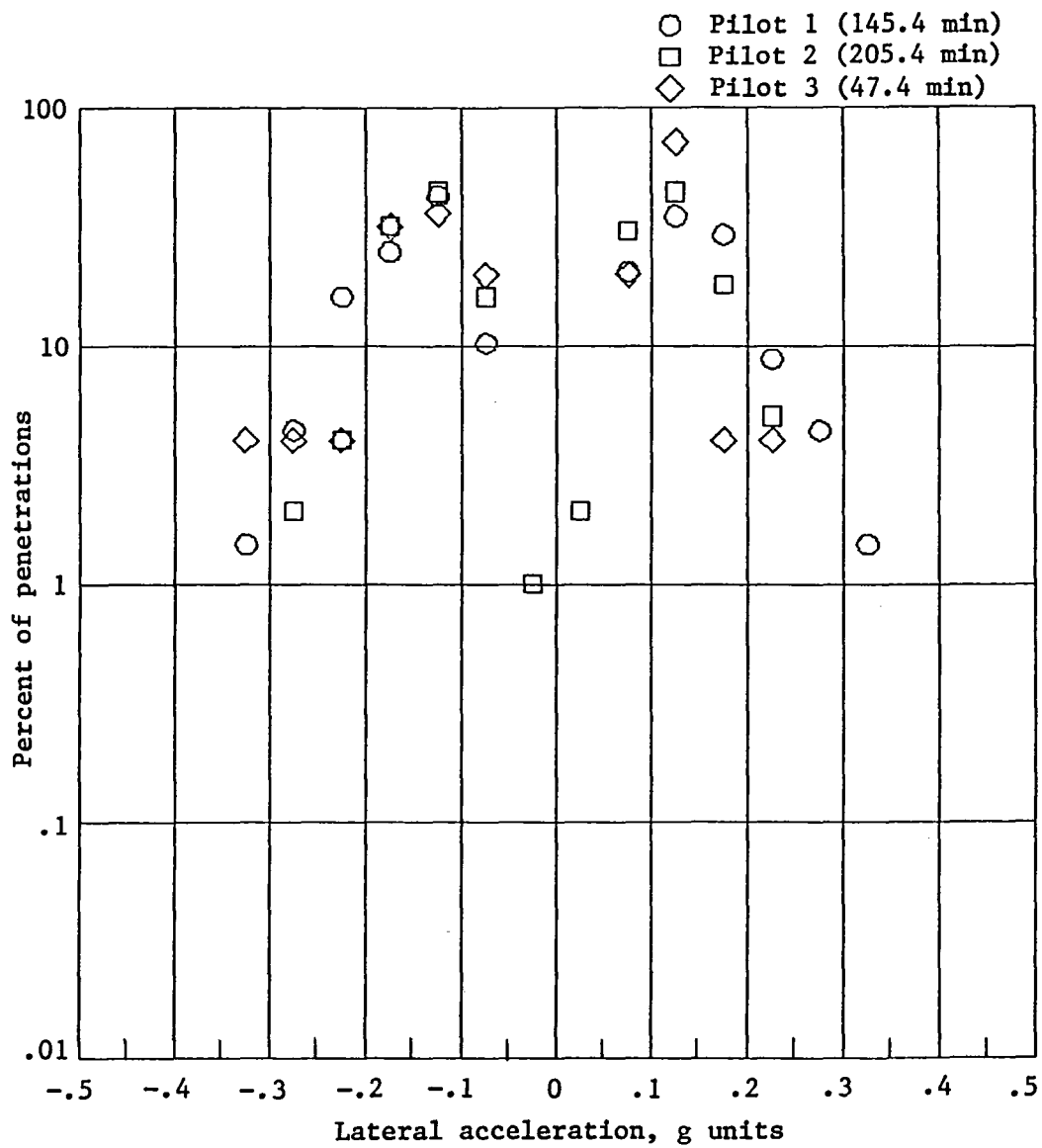
Figure 5.- Continued.

All pilots (398.1 min)



(c) Peak positive and negative occurrences per storm penetration for all data.

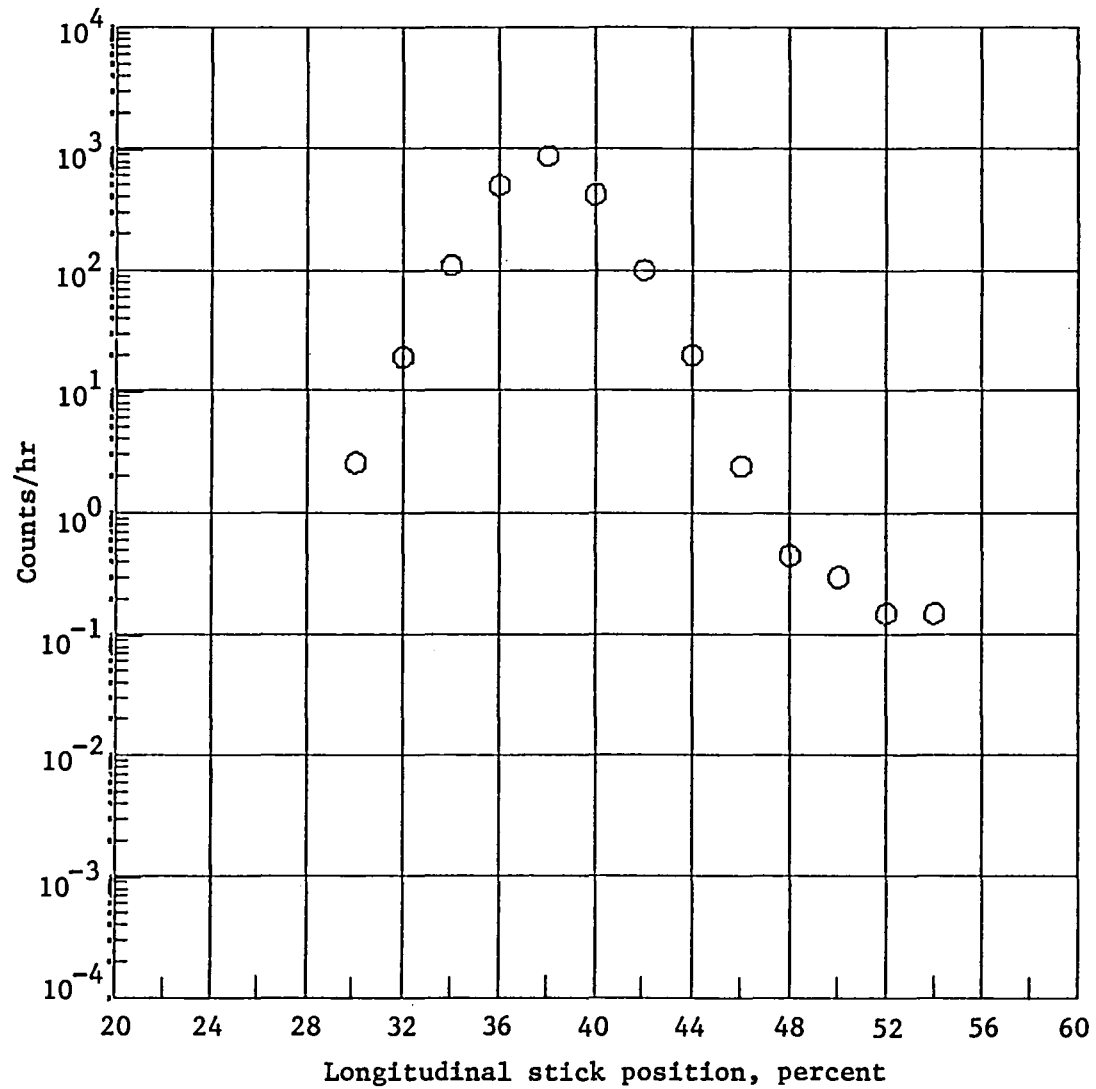
Figure 5.- Continued.



(d) Peak positive and negative occurrences per storm penetration for each pilot.

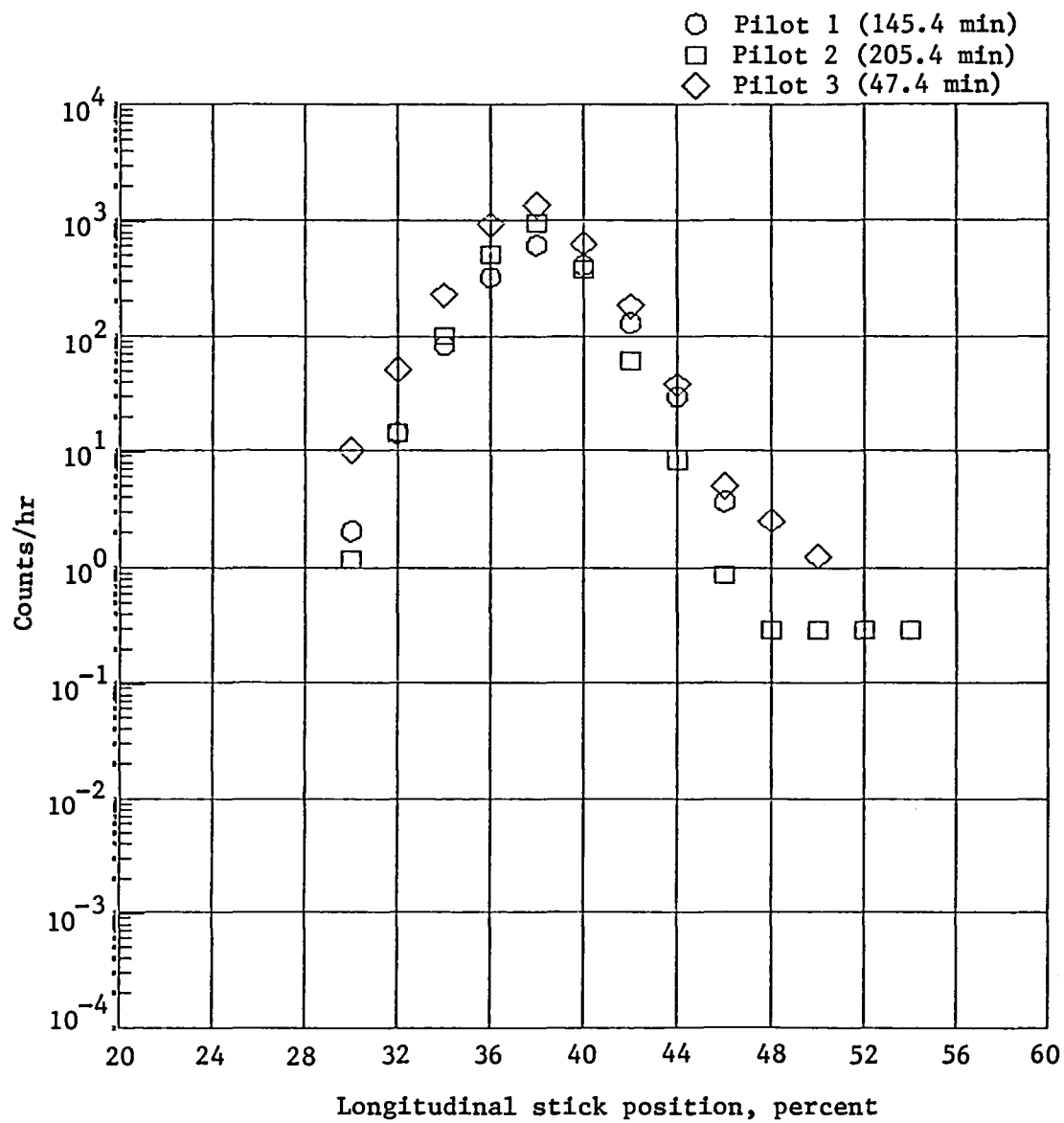
Figure 5.- Concluded.

All pilots (398.1 min)



(a) Level crossing rates for all data.

Figure 6.- Longitudinal stick movement during thunderstorm penetrations.

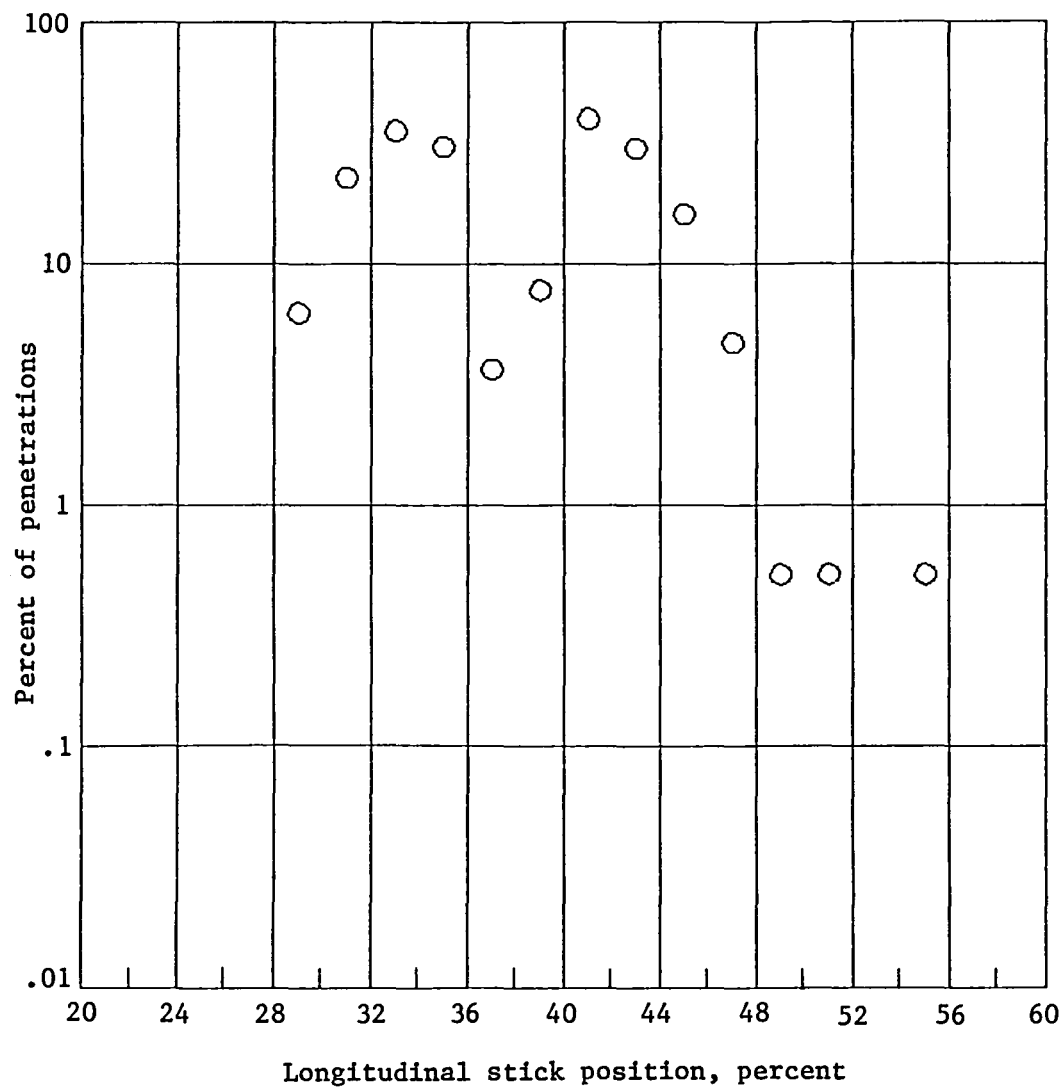


(b) Level crossing rates for each pilot.

Figure 6.- Continued.

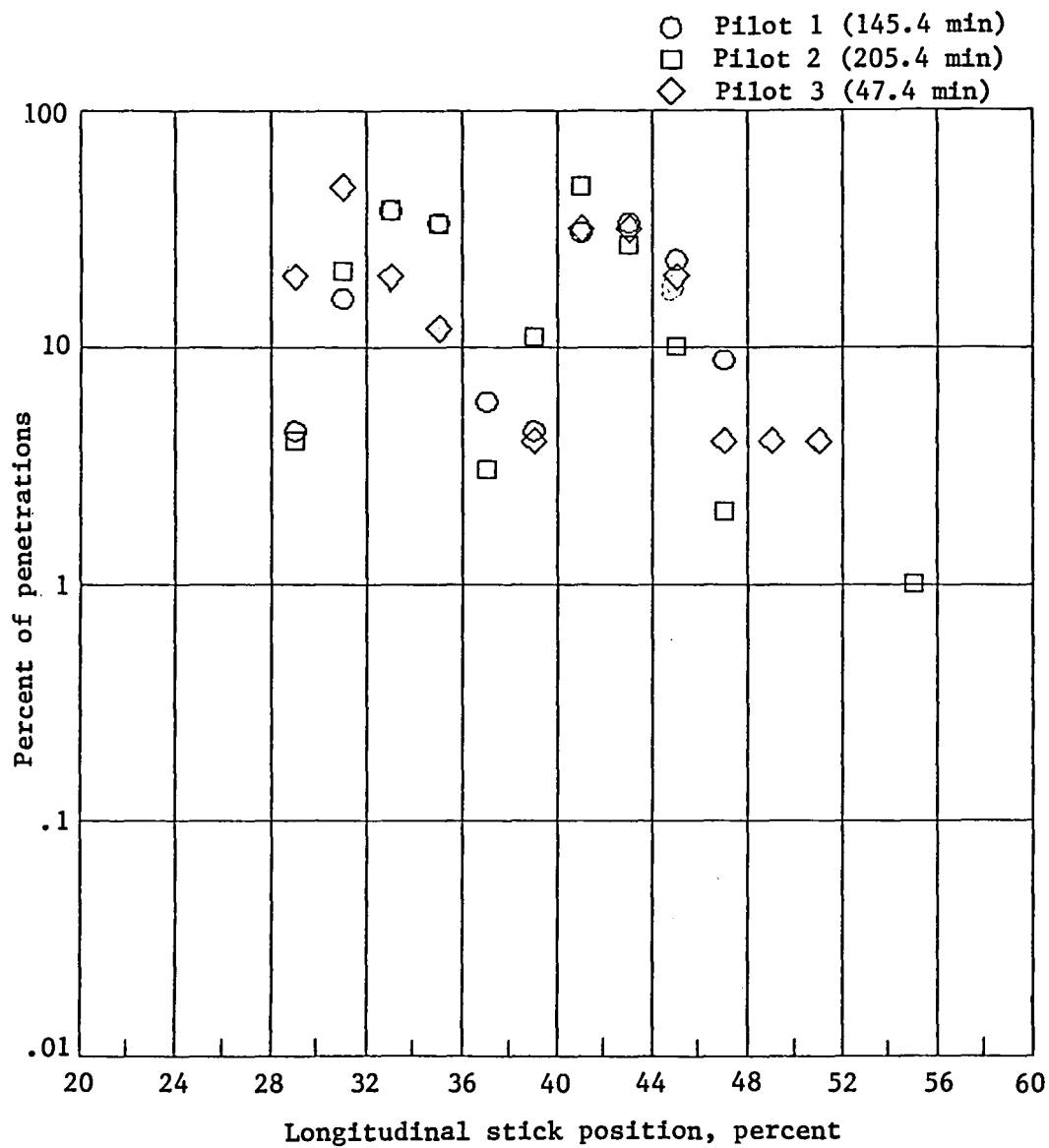


All pilots (398.1 min)



(c) Peak positive and negative occurrences per storm penetration for all data.

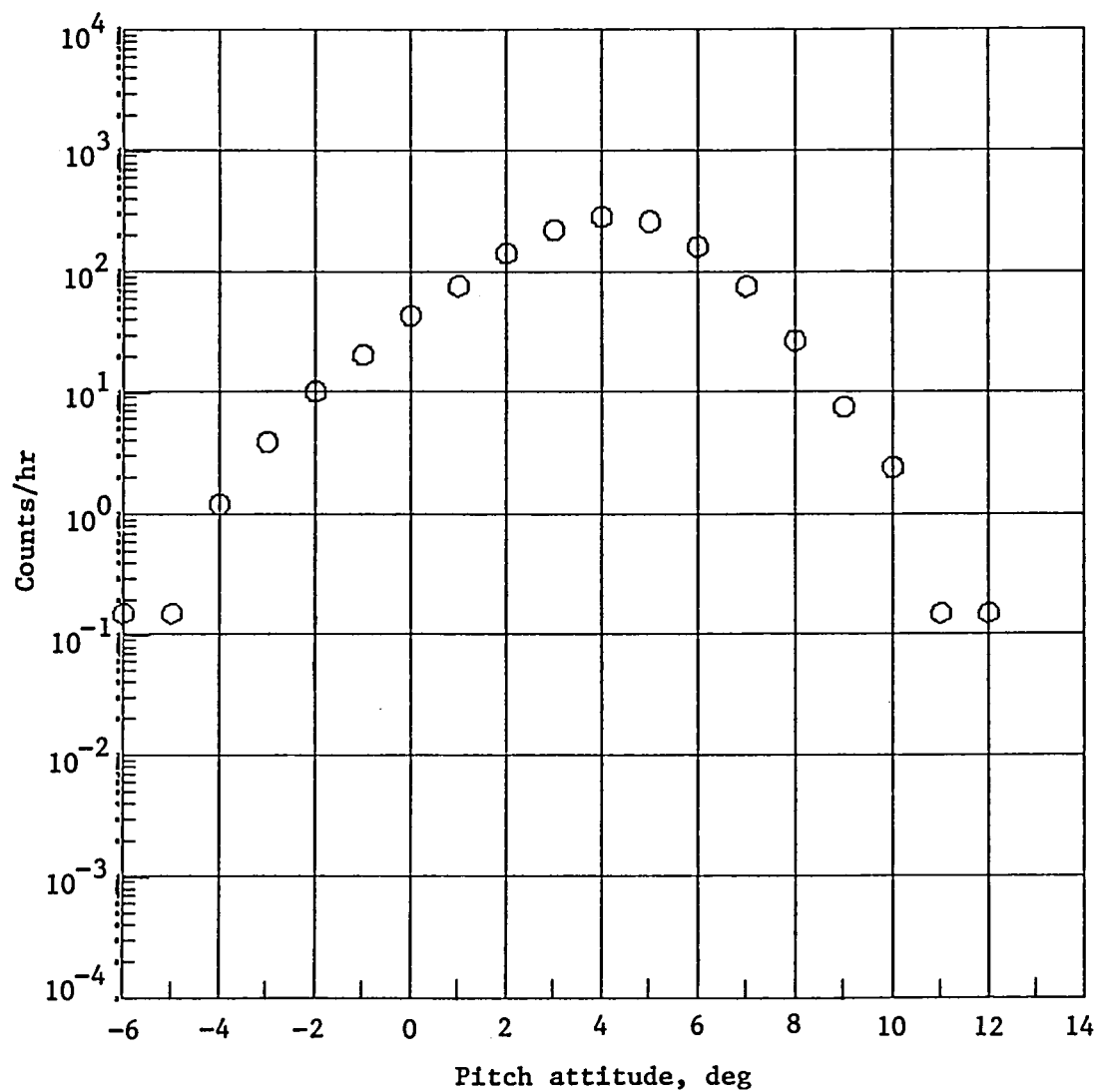
Figure 6.- Continued.



(d) Peak positive and negative occurrences per storm penetration for each pilot.

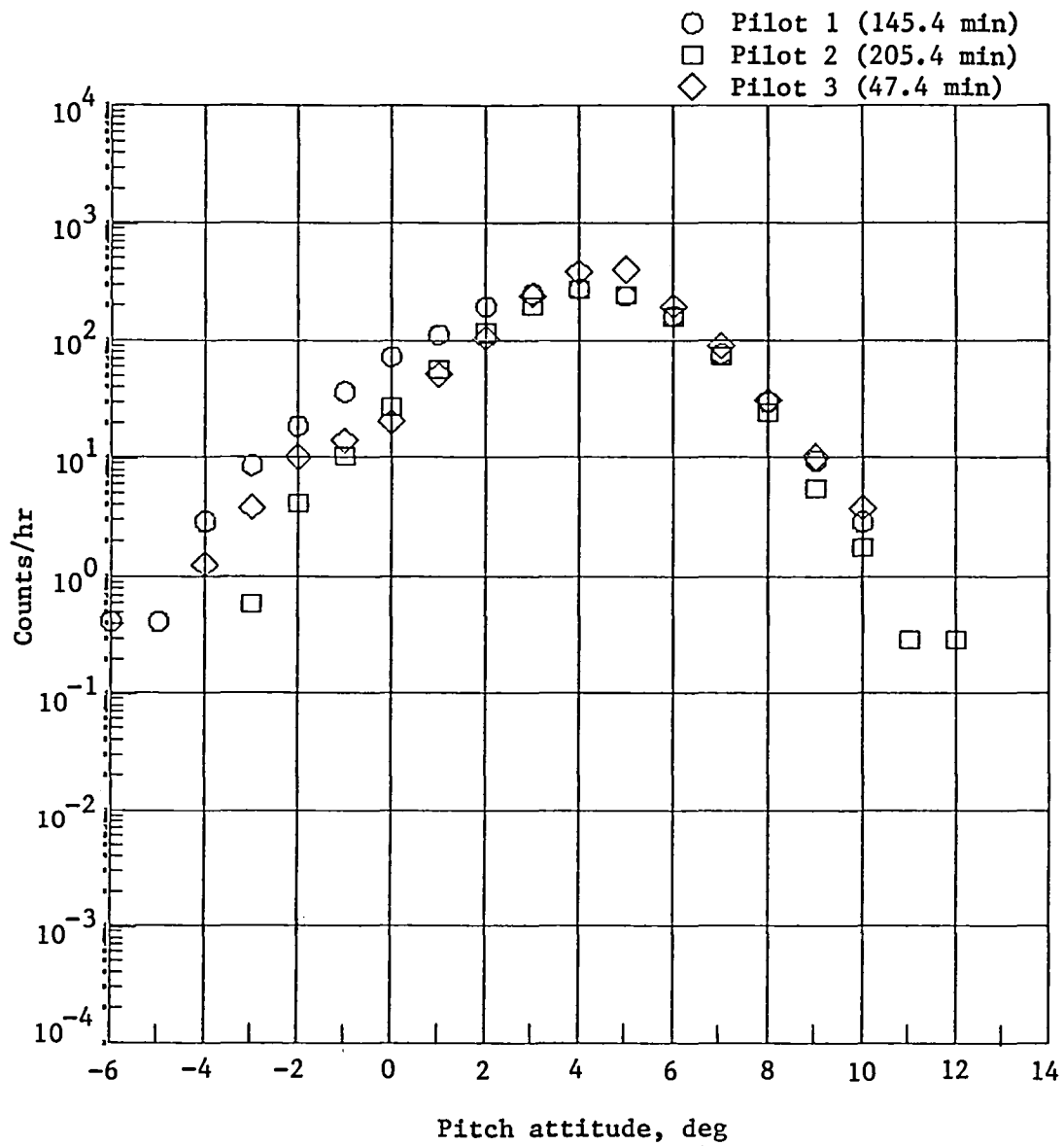
Figure 6.- Concluded.

All pilots (398.1 min)



(a) Level crossing rates for all data.

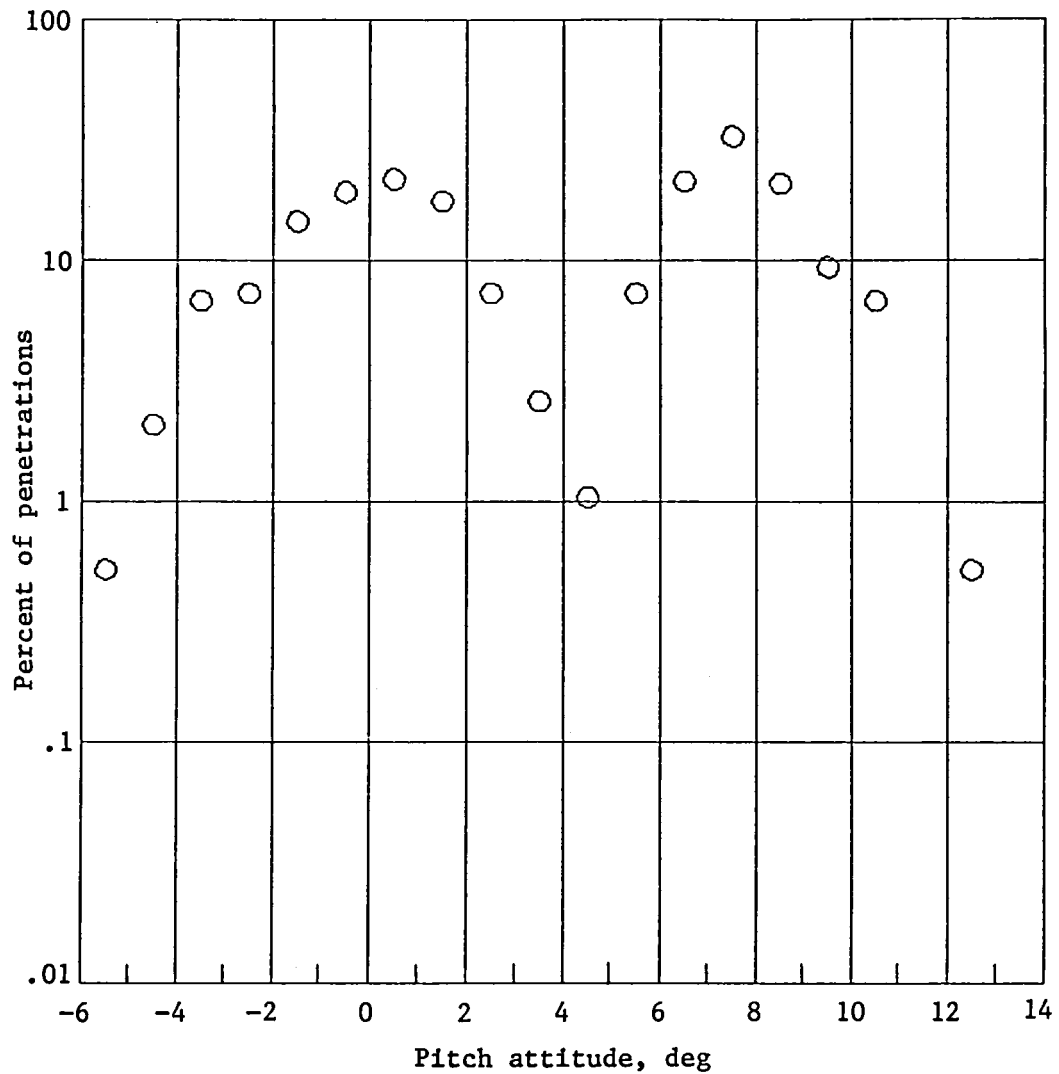
Figure 7.- F-106B pitch attitude during thunderstorm penetrations.



(b) Level crossing rates for each pilot.

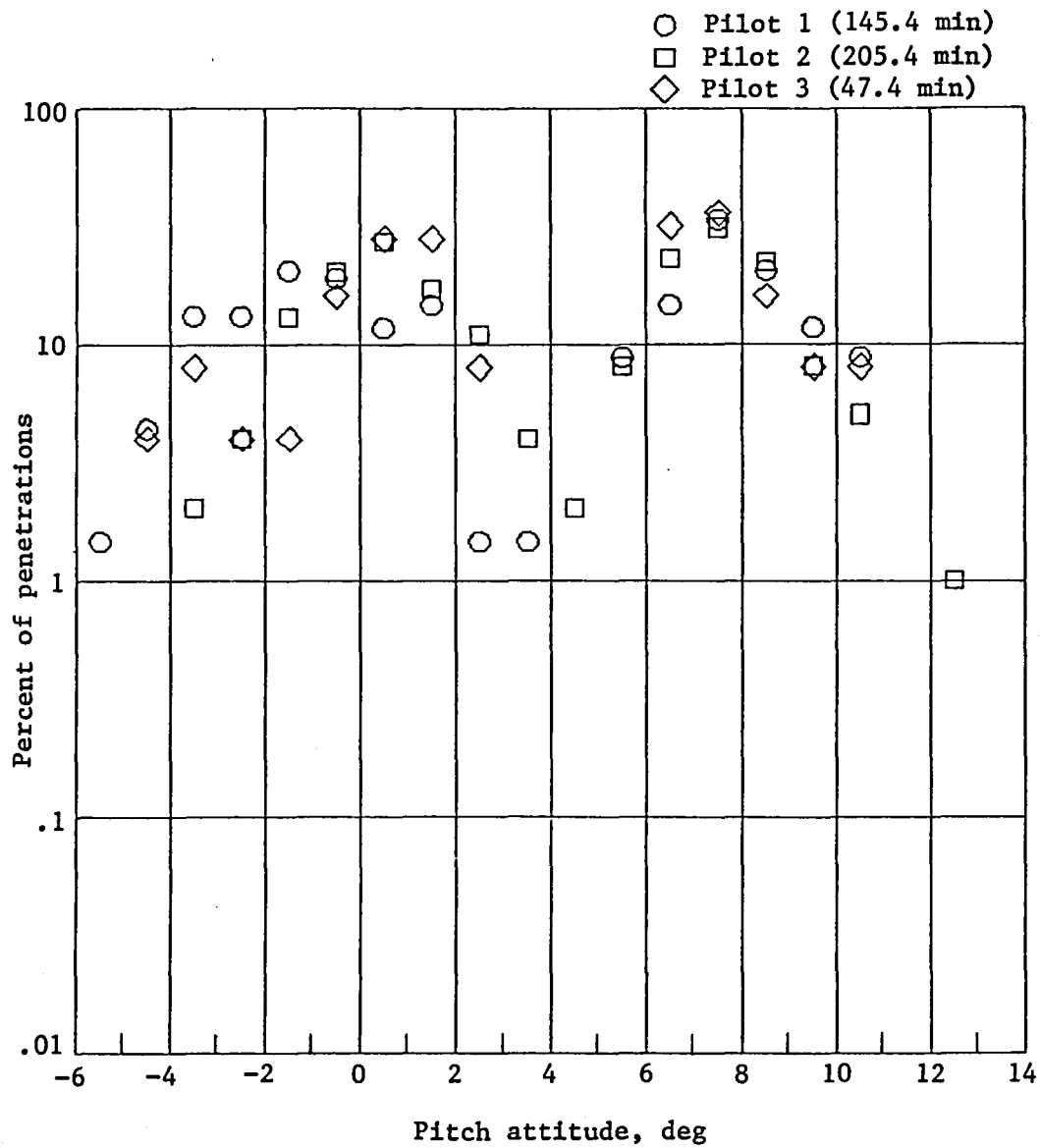
Figure 7.- Continued.

All pilots (398.1 min)



(c) Peak positive and negative occurrences per storm penetration for all data.

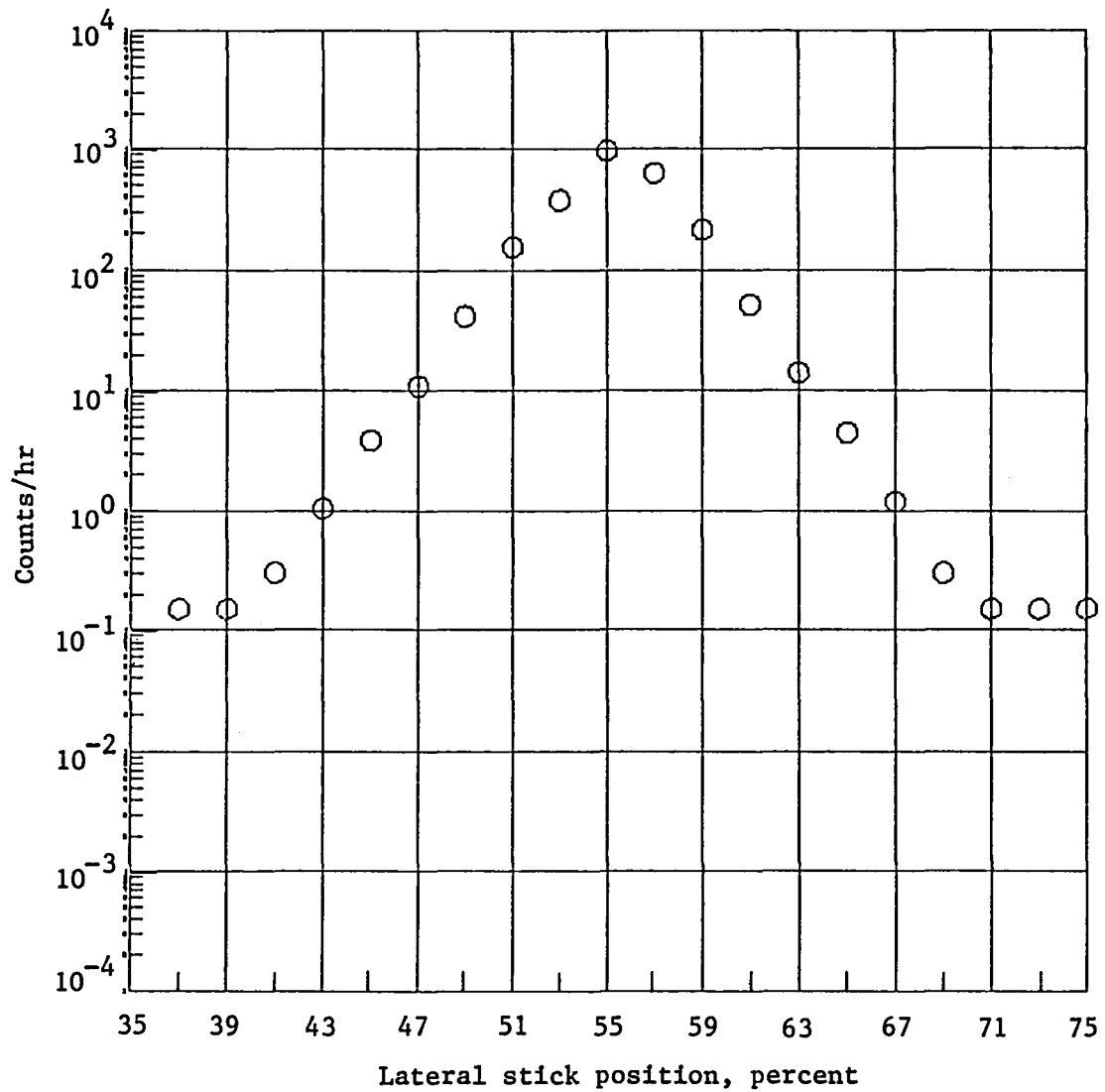
Figure 7.- Continued.



(d) Peak positive and negative occurrences per storm penetration for each pilot.

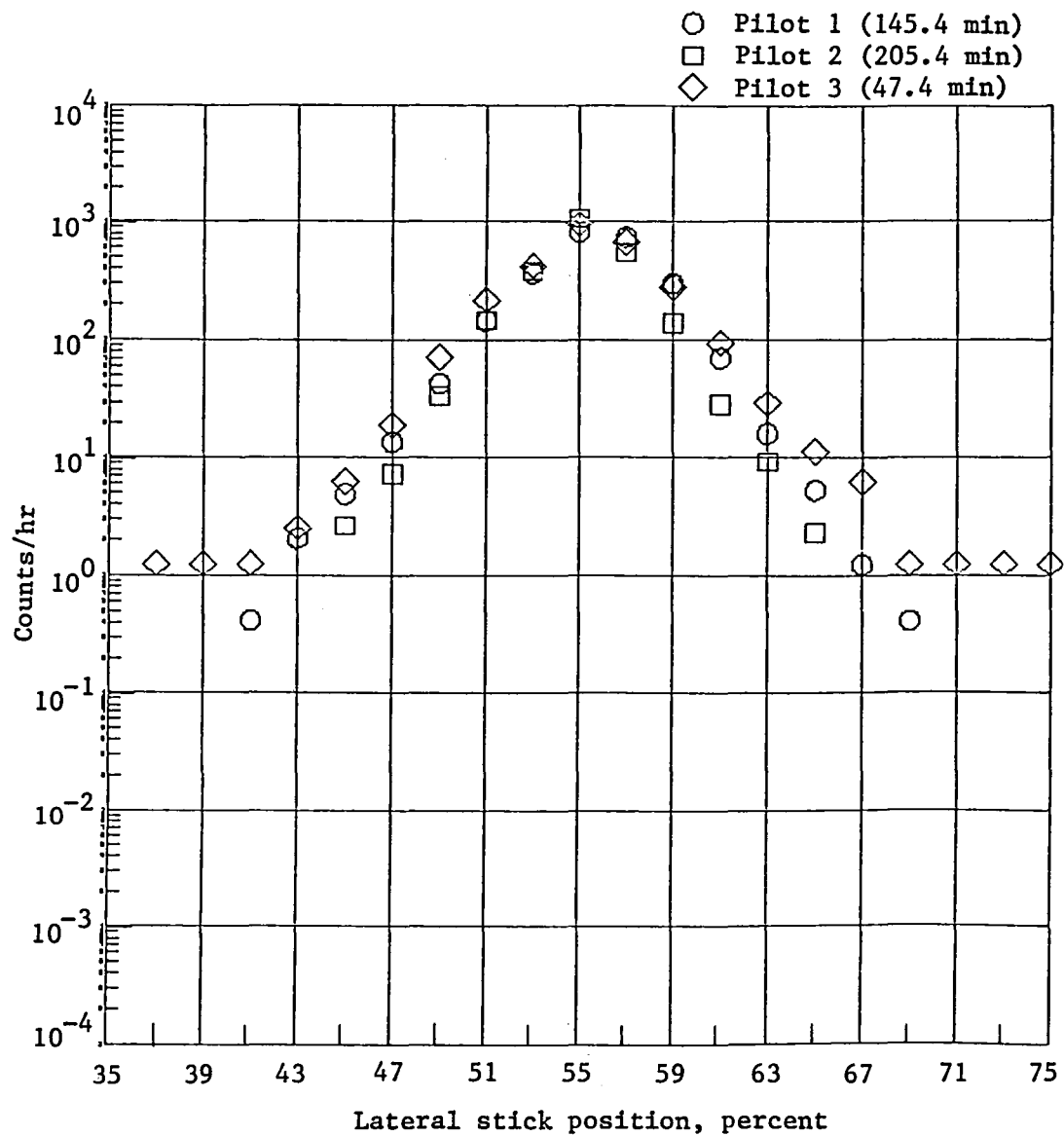
Figure 7.- Concluded.

All pilots (398.1 min)



(a) Level crossing rates for all data.

Figure 8.- Lateral stick movement during thunderstorm penetrations.

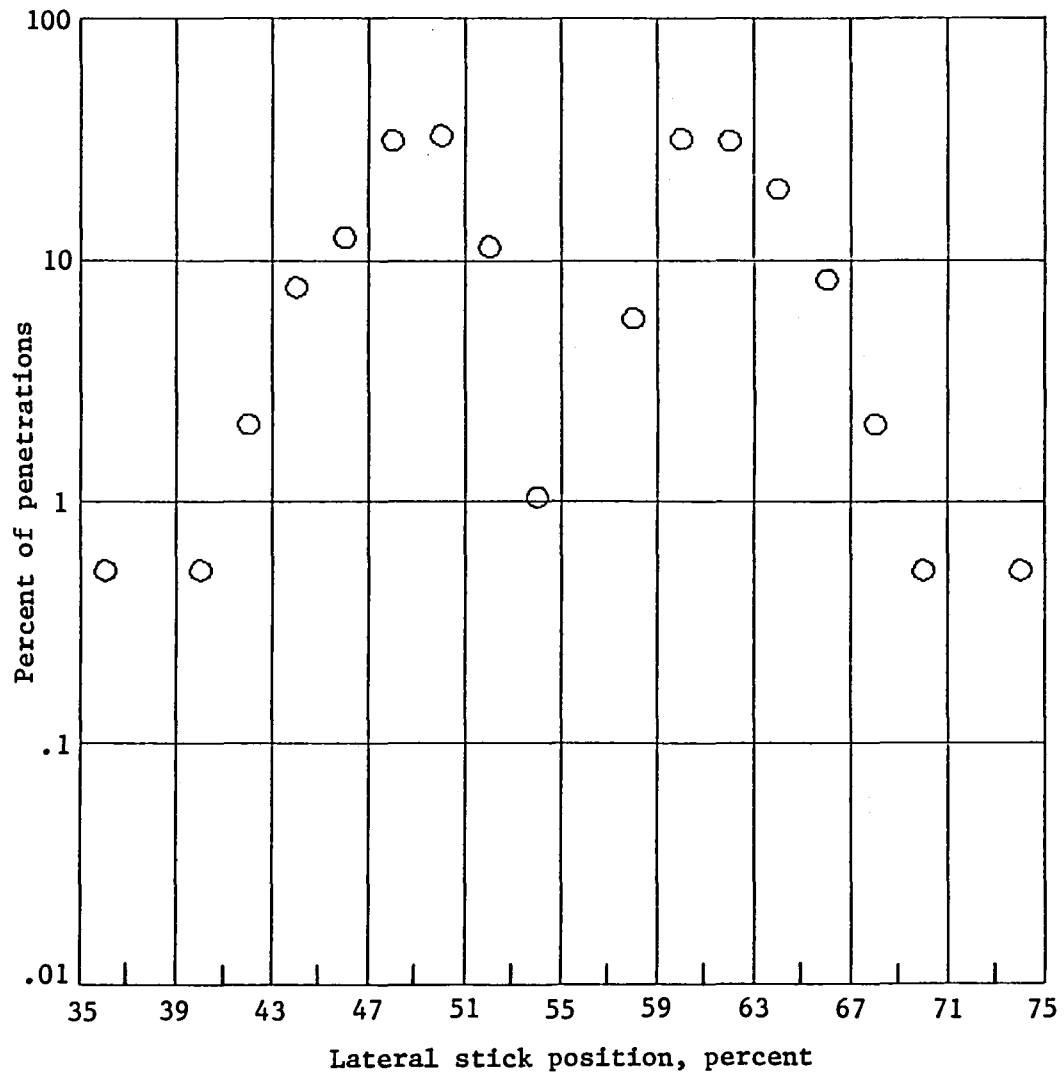


(b) Level crossing rates for each pilot.

Figure 8.- Continued.

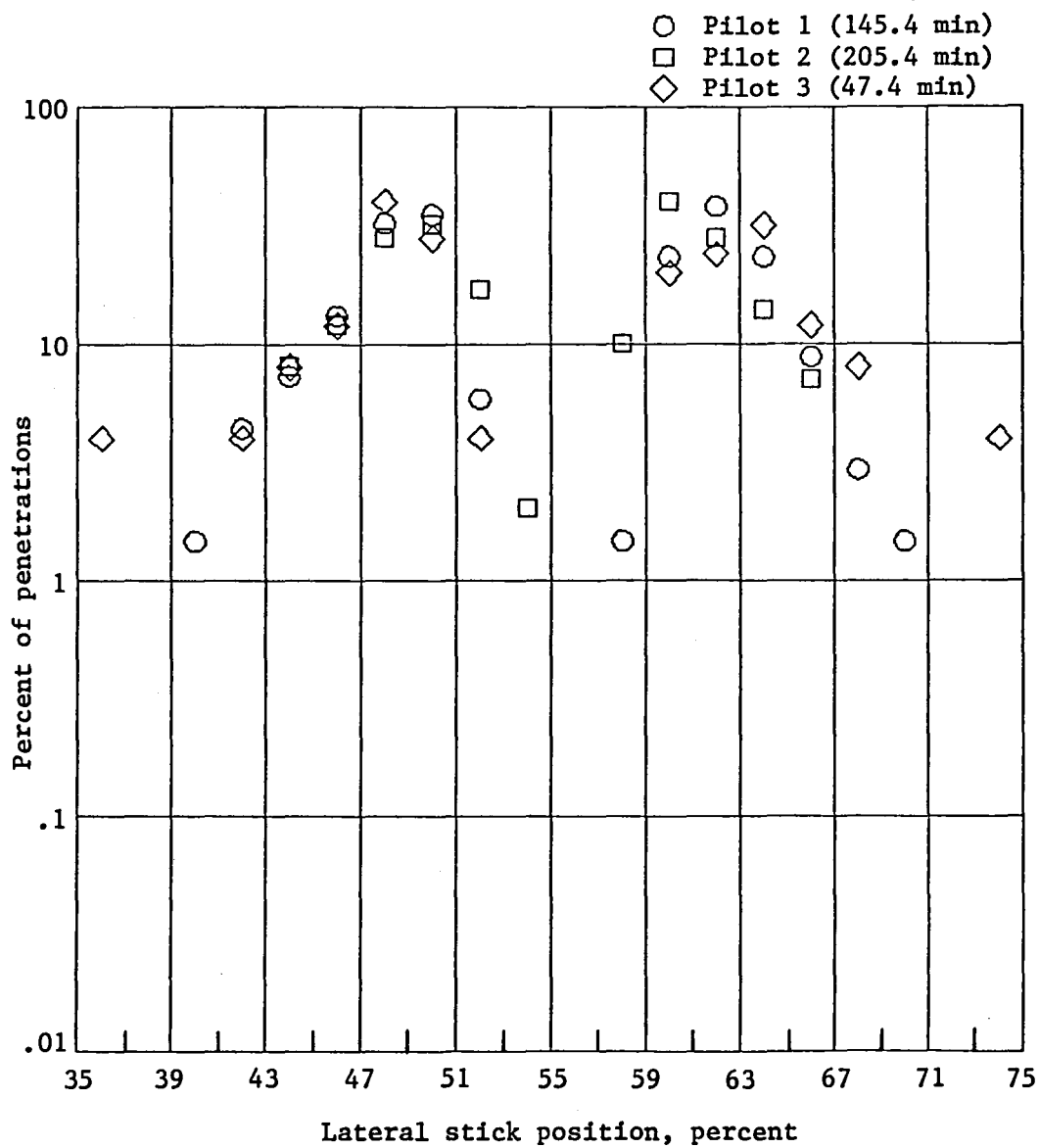


All pilots (398.1 min)



(c) Peak positive and negative occurrences per storm penetration for all data.

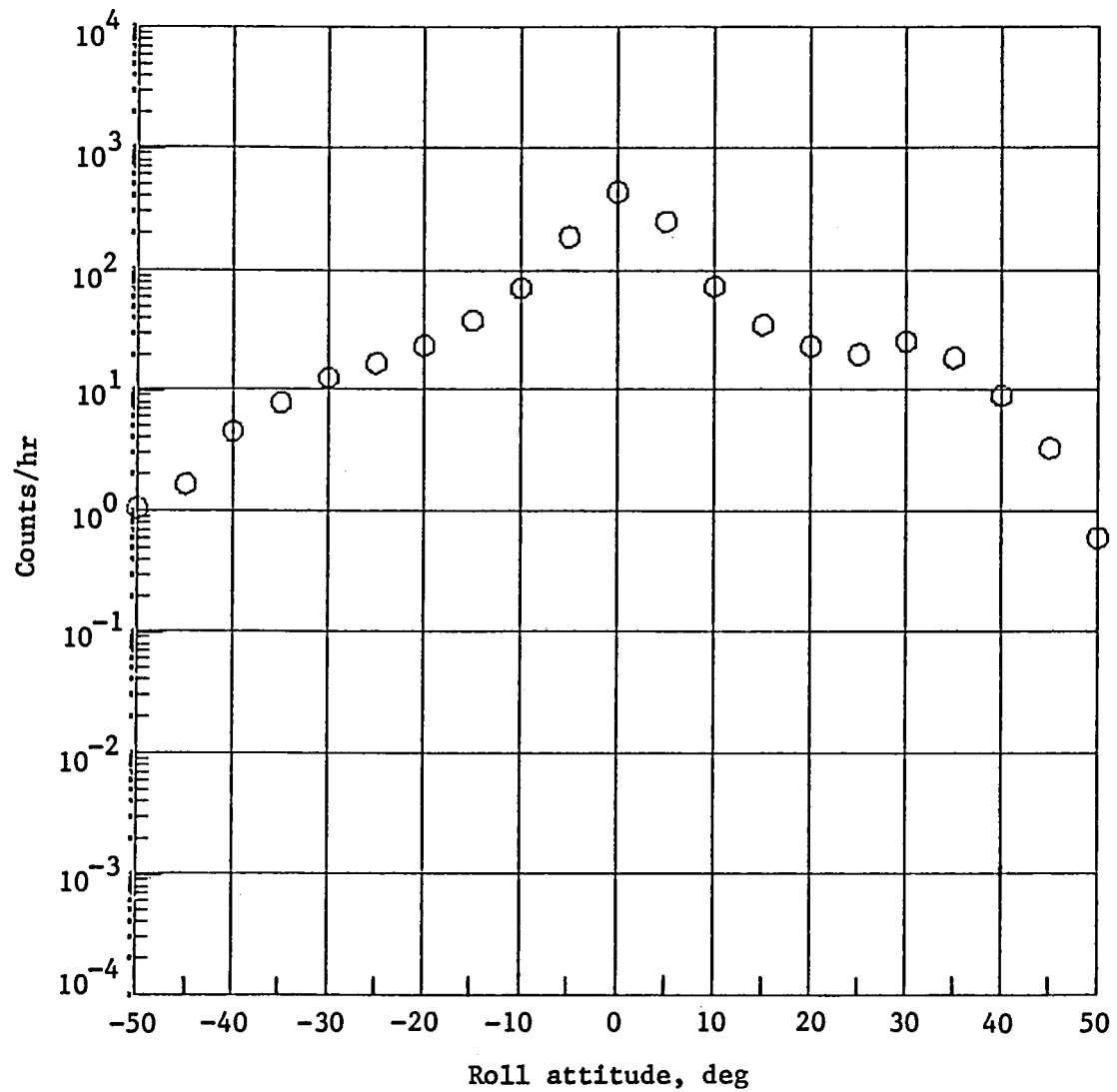
Figure 8.- Continued.



(d) Peak positive and negative occurrences per storm penetration for each pilot.

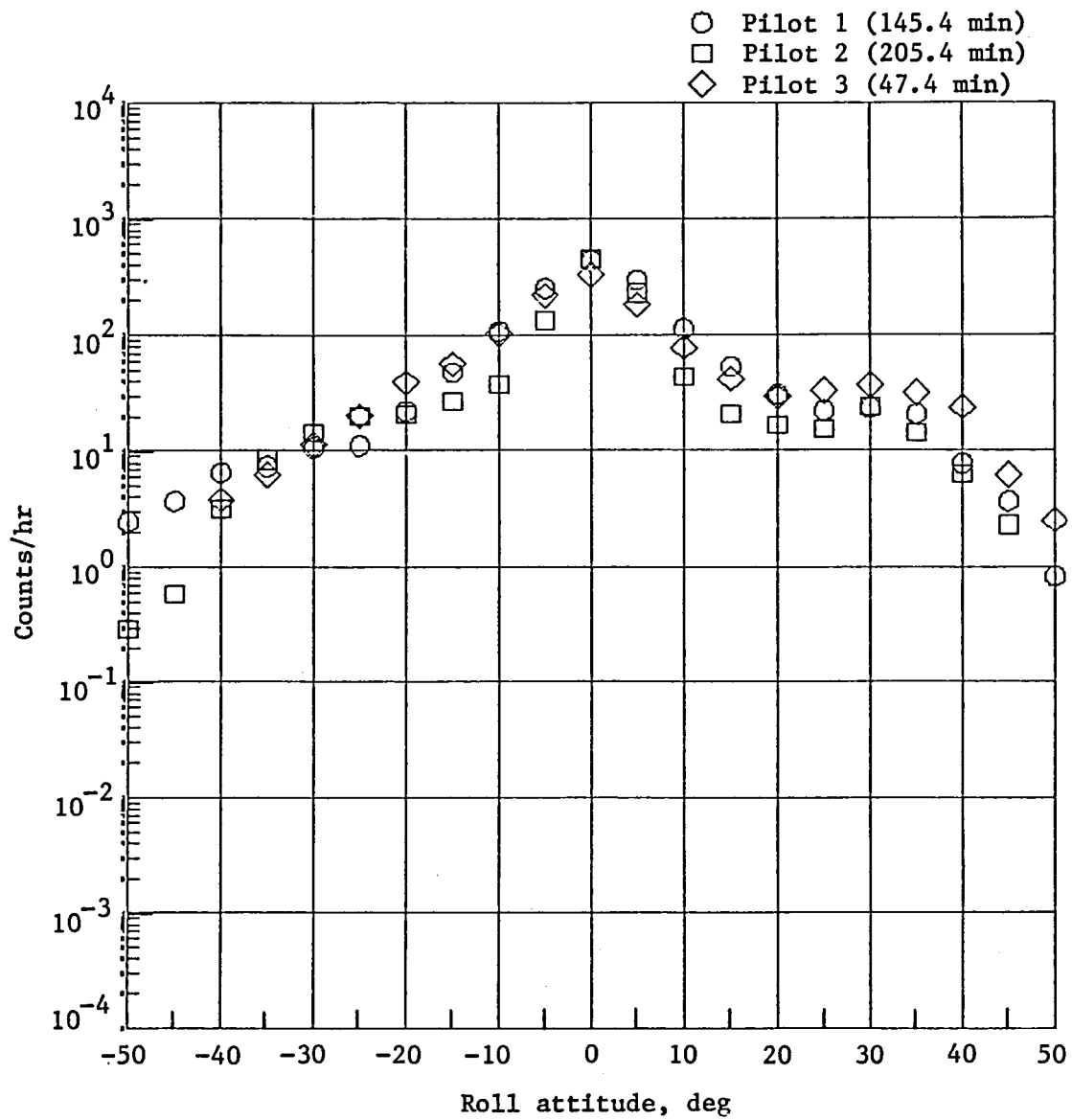
Figure 8.- Concluded.

All pilots (398.1 min)



(a) Level crossing rates for all data.

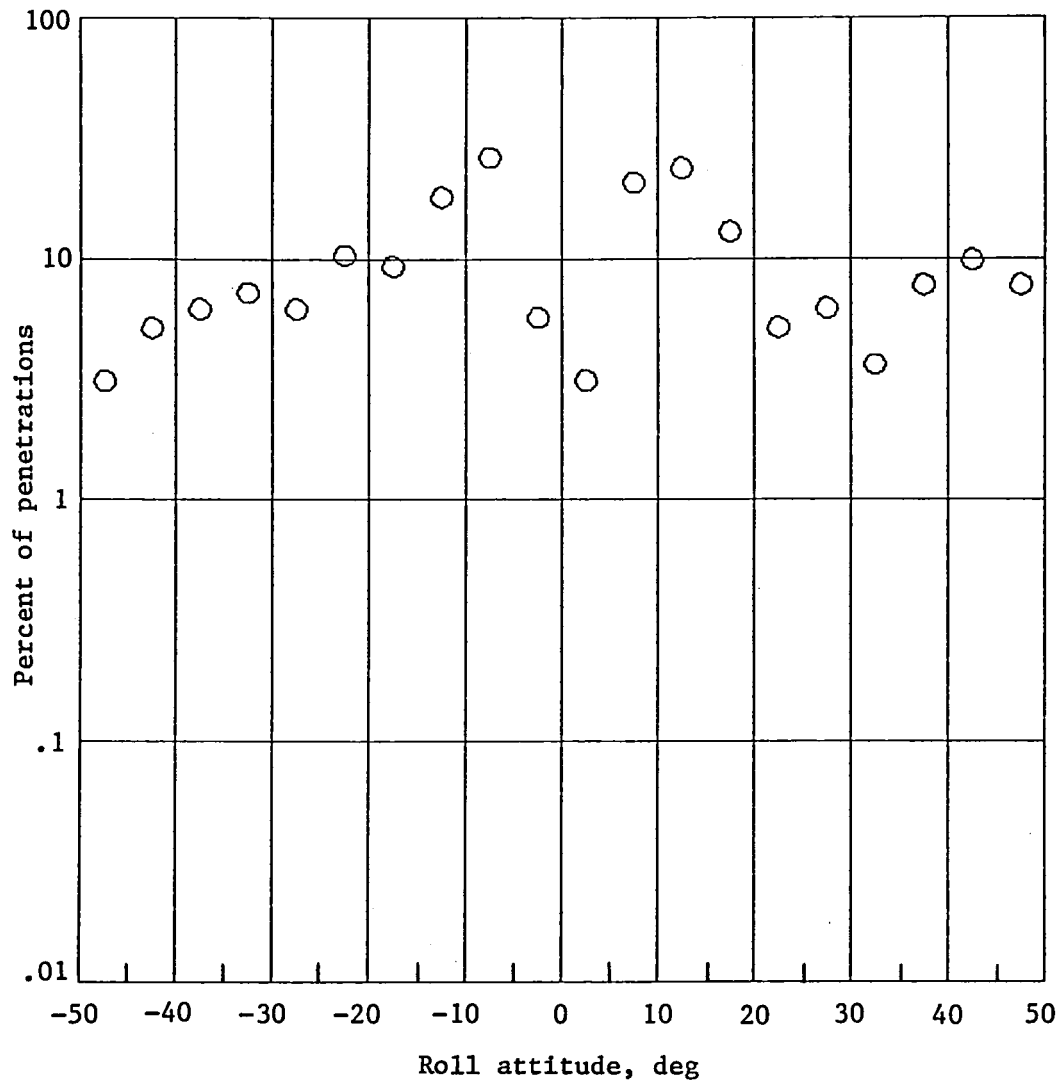
Figure 9.- F-106B roll attitude during thunderstorm penetrations.



(b) Level crossing rates for each pilot.

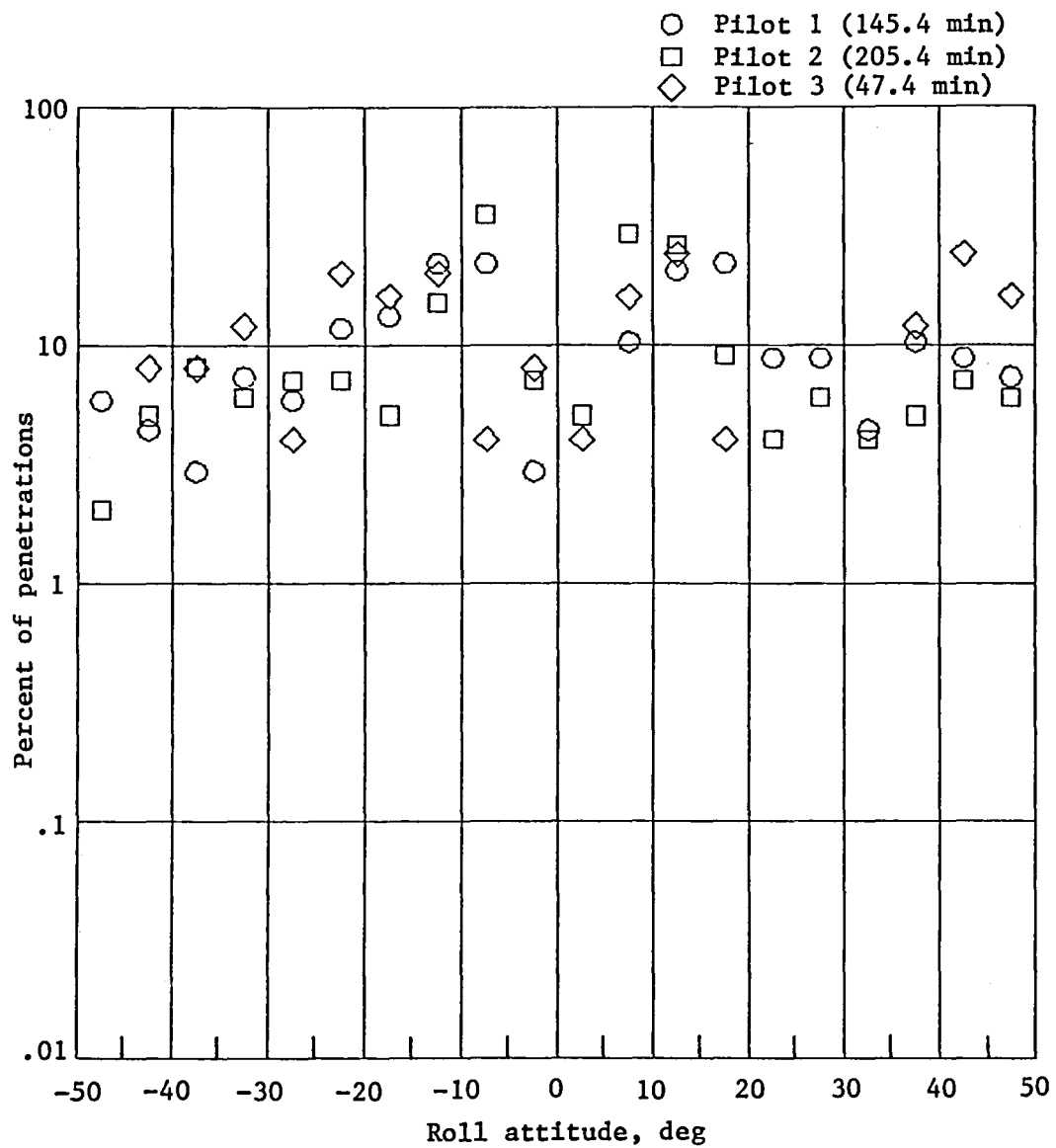
Figure 9.- Continued.

All pilots (398.1 min)



(c) Peak positive and negative occurrences per storm penetration for all data.

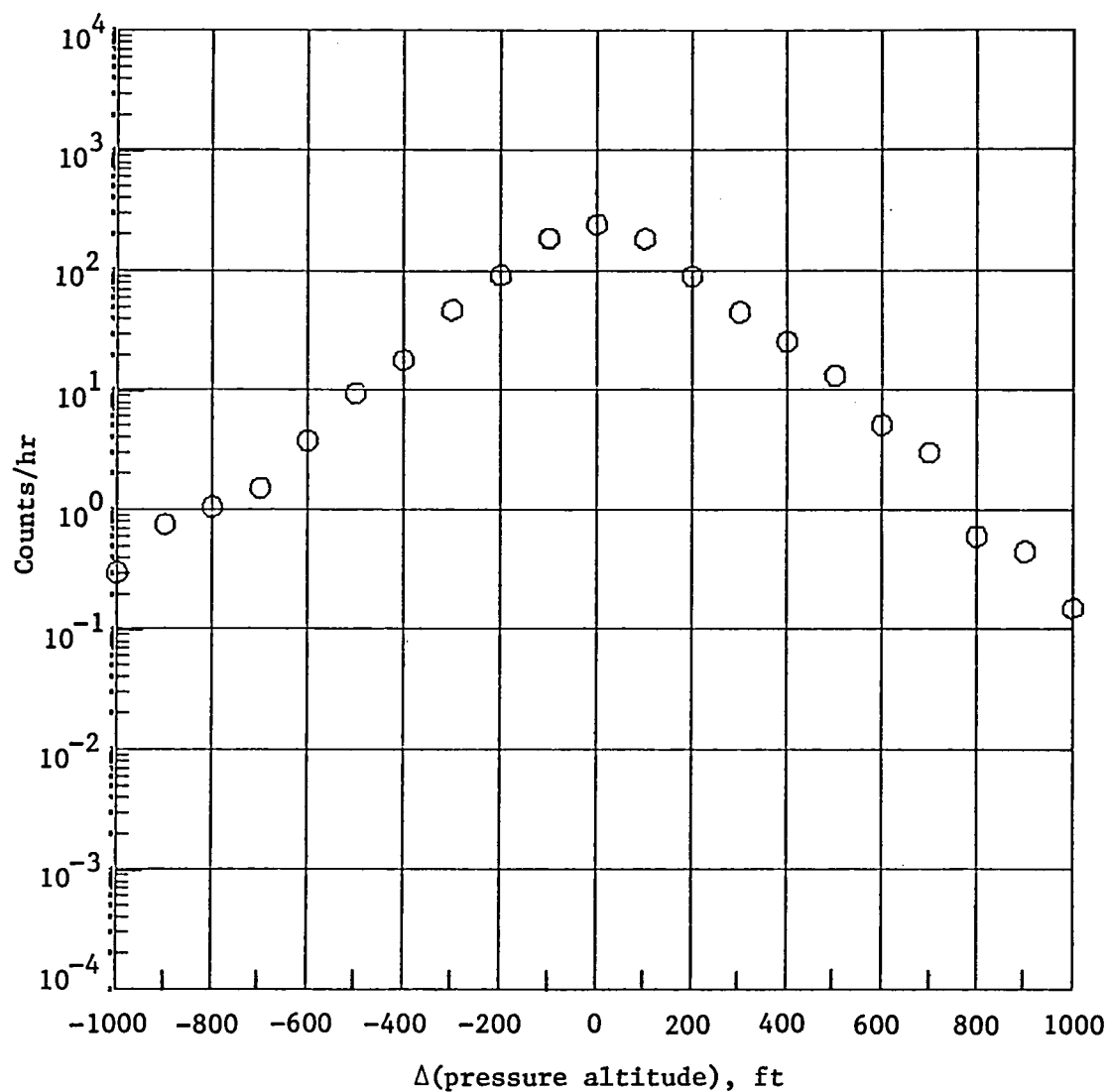
Figure 9.- Continued.



(d) Peak positive and negative occurrences per storm penetration for each pilot.

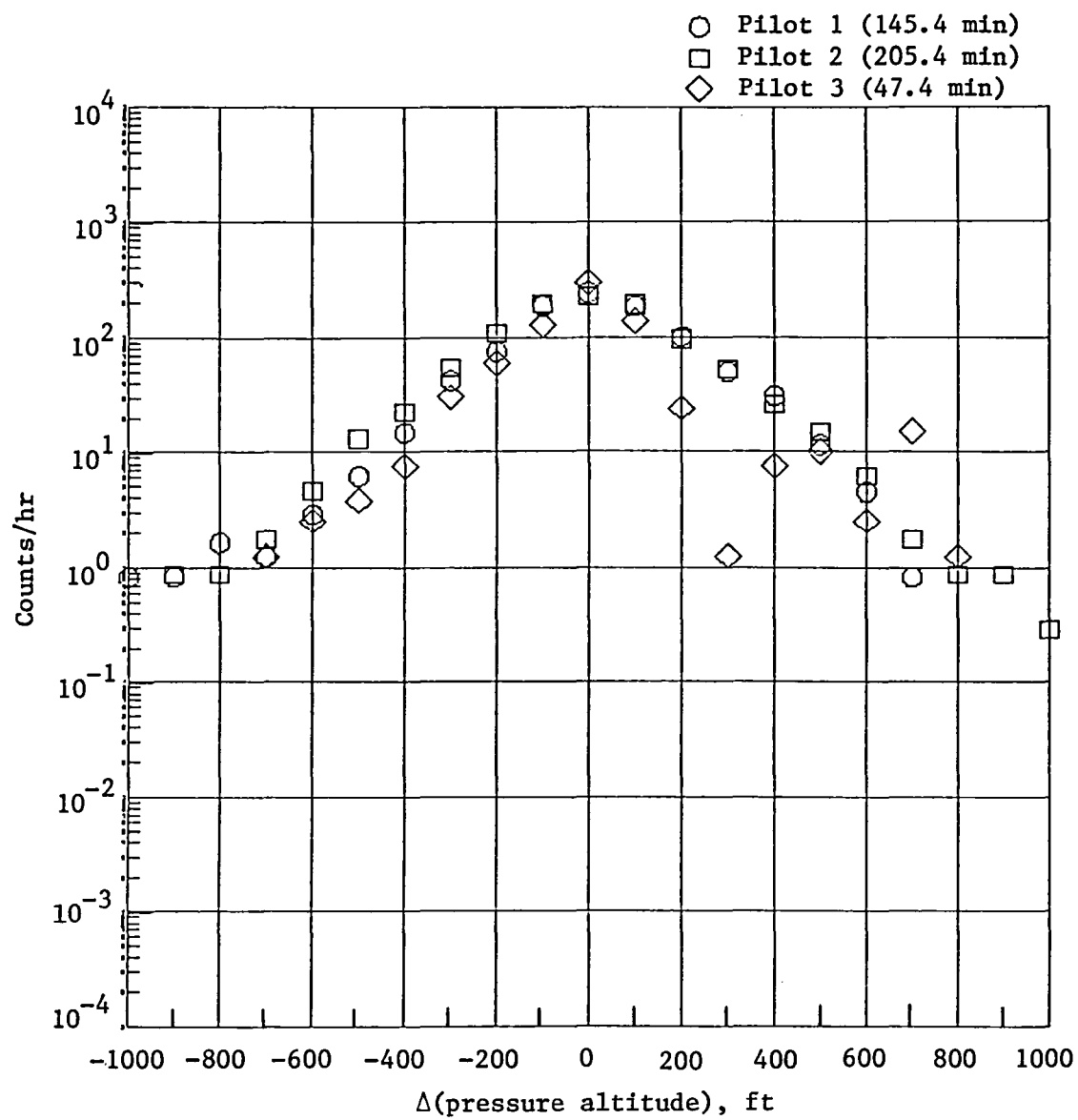
Figure 9.- Concluded.

All pilots (398.1 min)



(a) Level crossing rates for all data.

Figure 10.- F-106B altitude variations during thunderstorm penetrations.

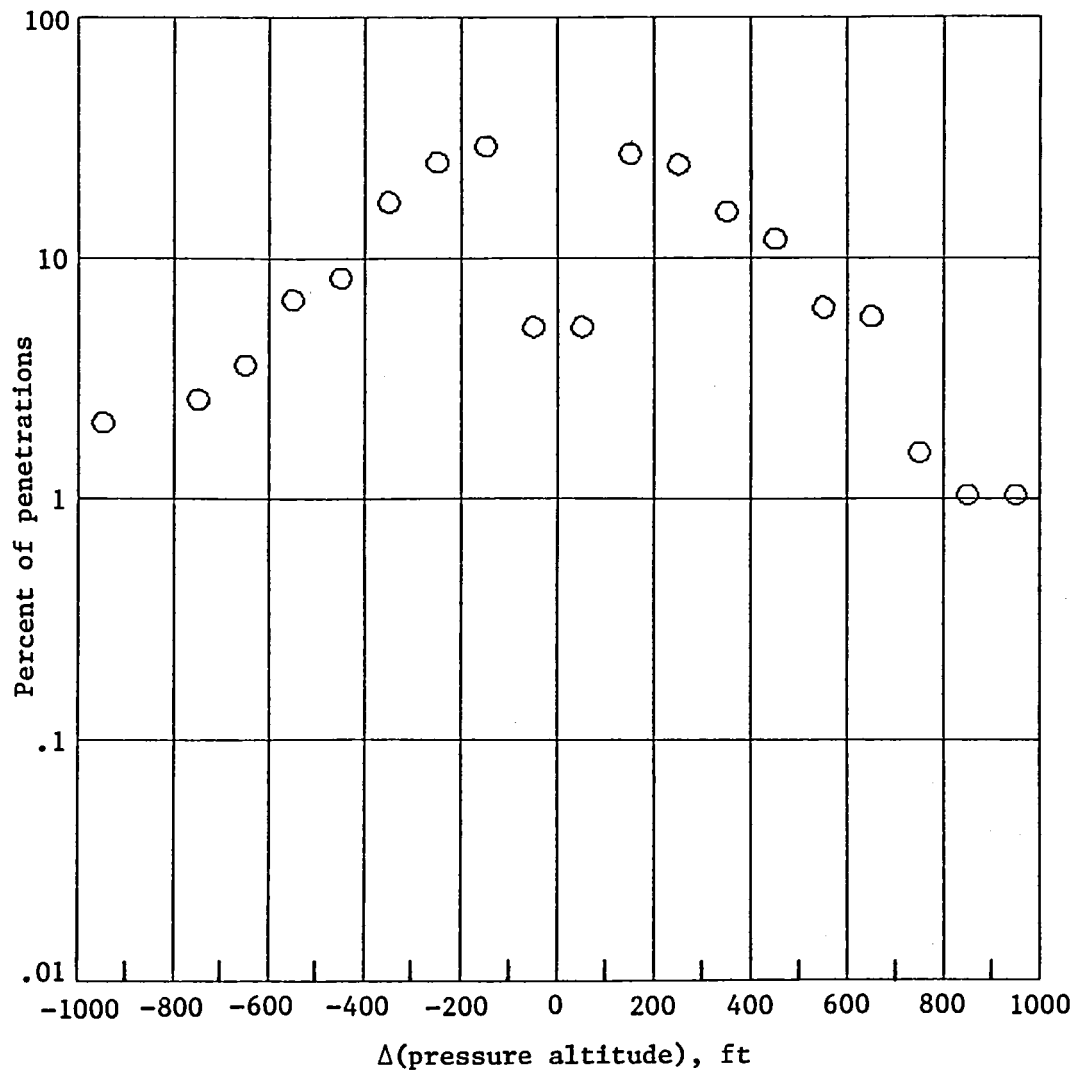


(b) Level crossing rates for each pilot.

Figure 10.- Continued.

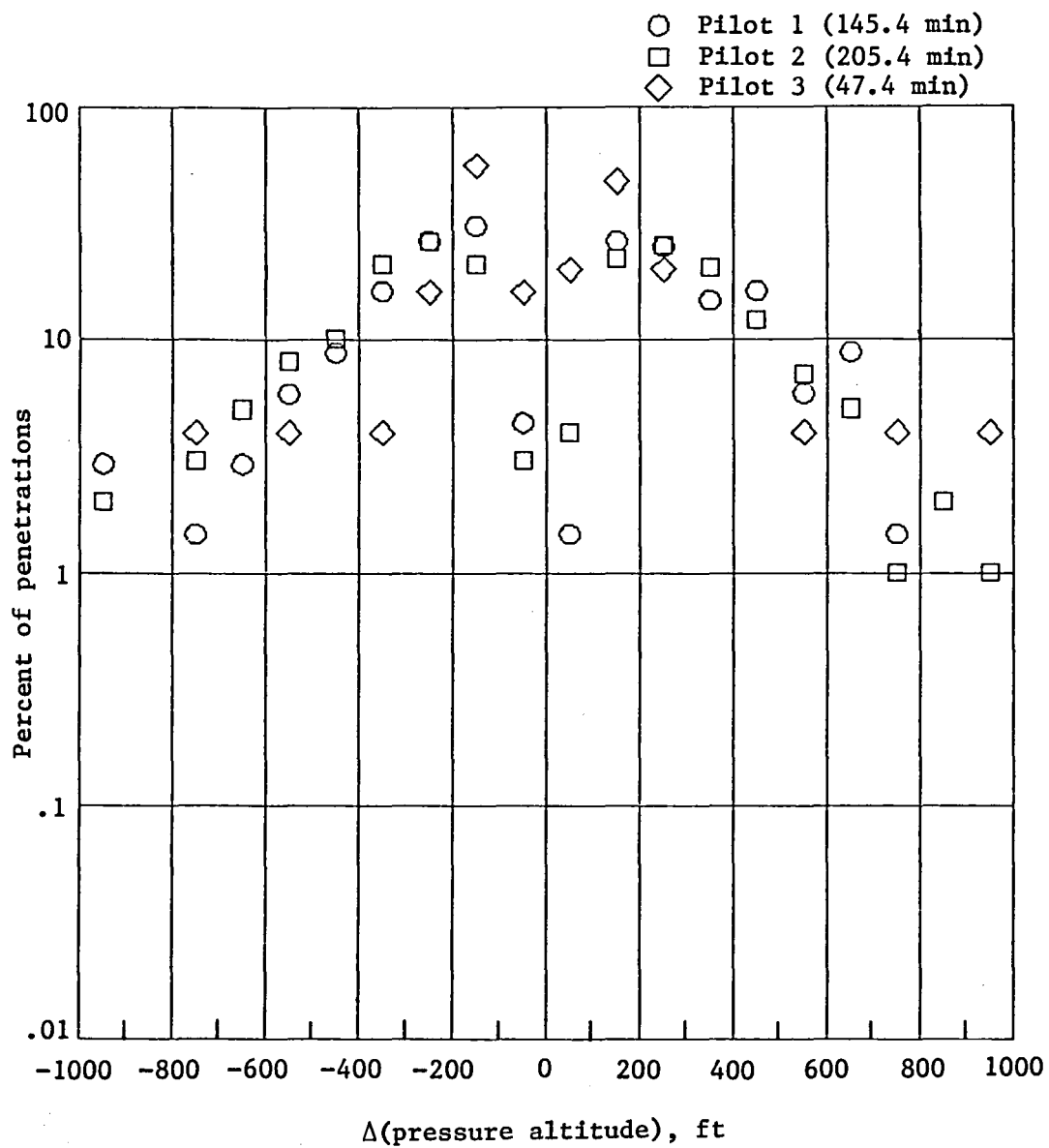


All pilots (398.1 min)



(c) Peak positive and negative occurrences per storm penetration for all data.

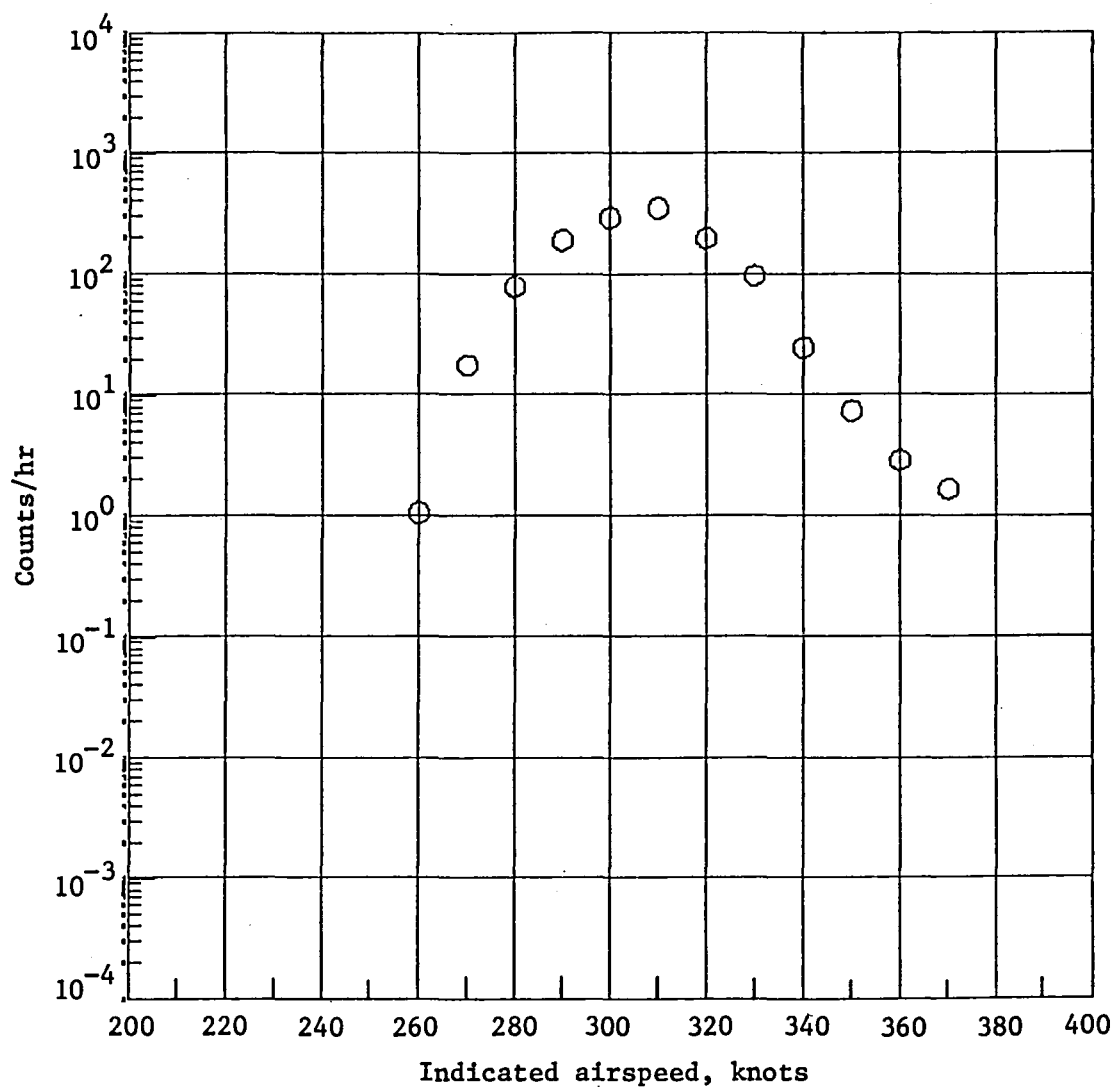
Figure 10.- Continued.



(d) Peak positive and negative occurrences per storm penetration for each pilot.

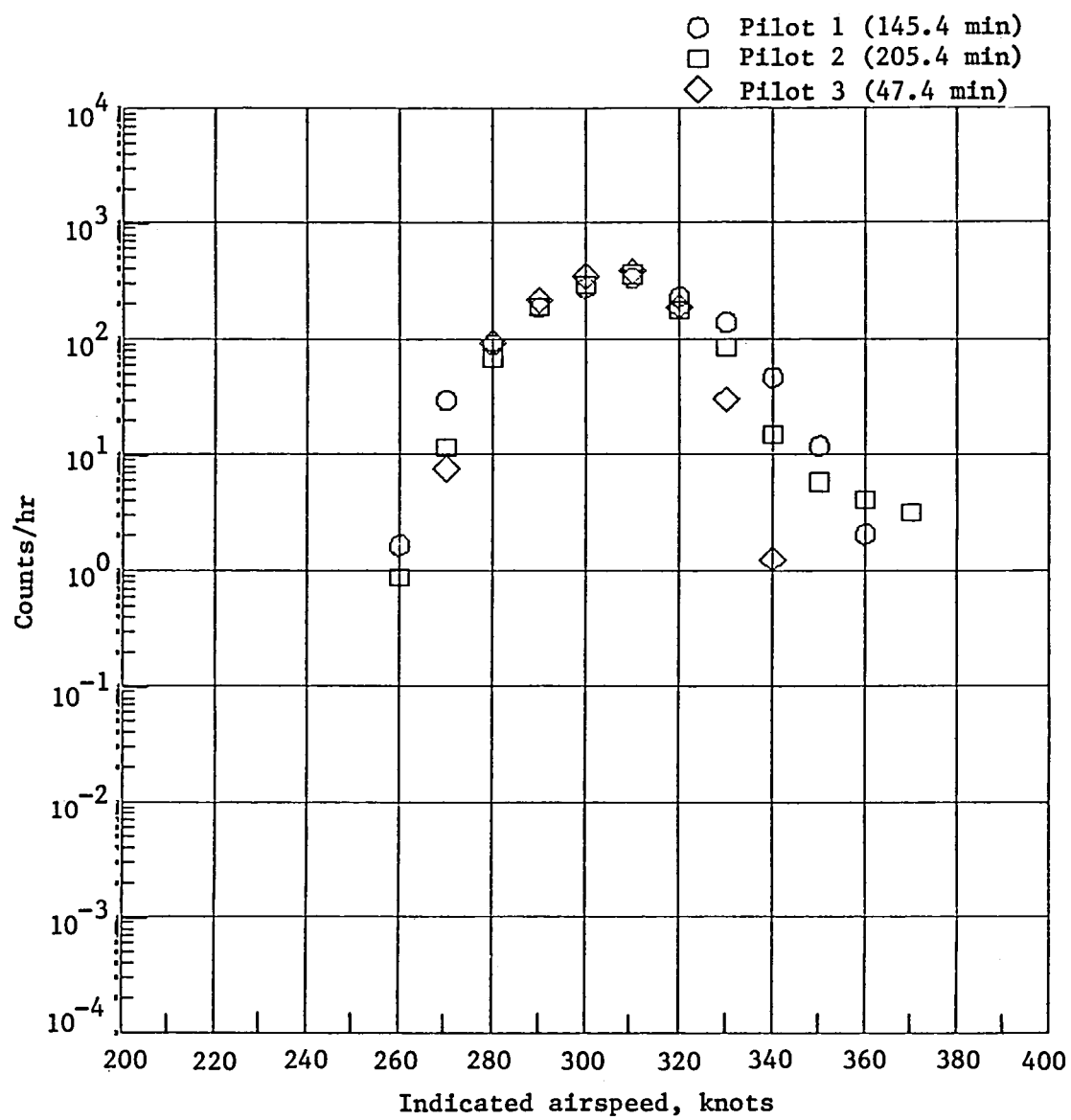
Figure 10.- Concluded.

All pilots (398.1 min)



(a) Level crossing rates for all data.

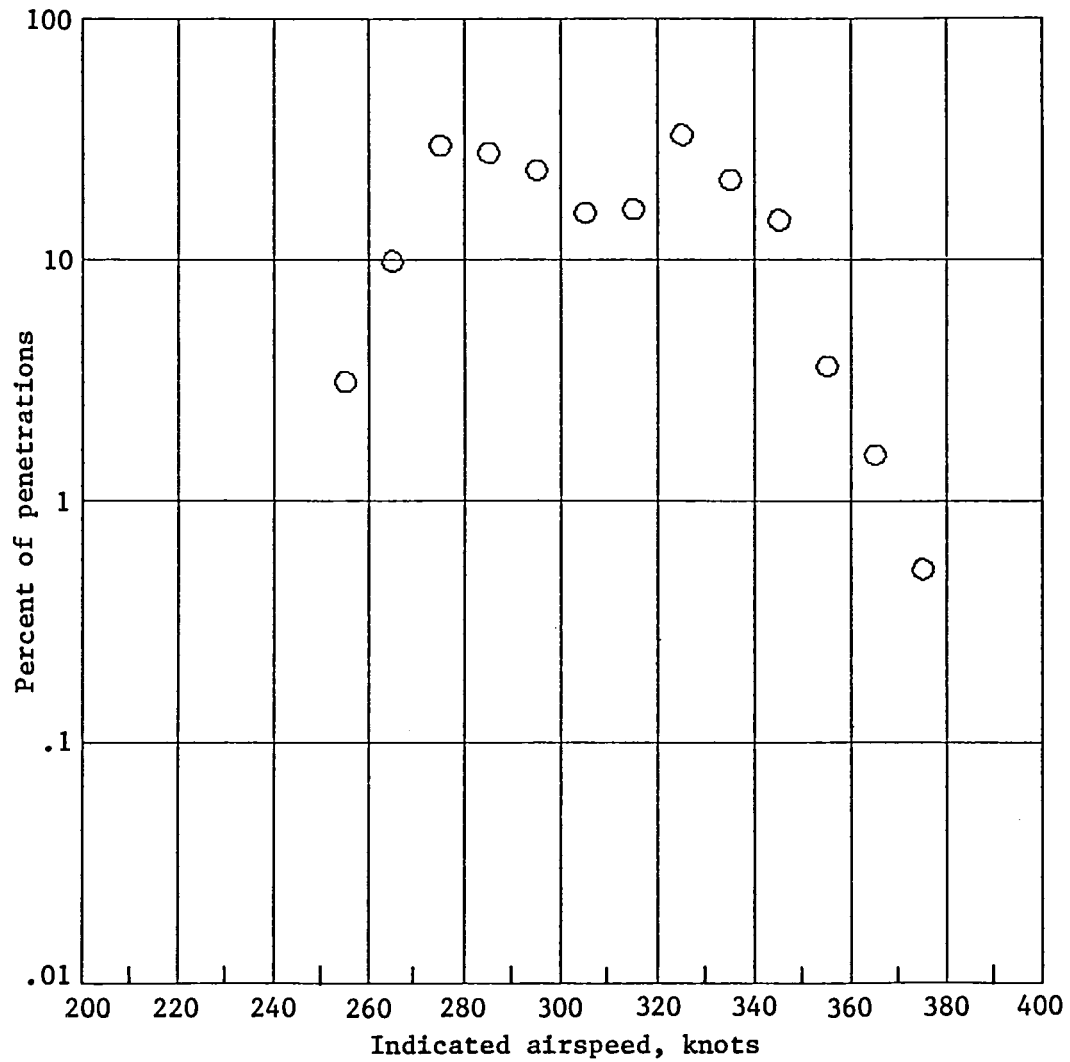
Figure 11.- Indicated airspeed variations during thunderstorm penetrations.



(b) Level crossing rates for each pilot.

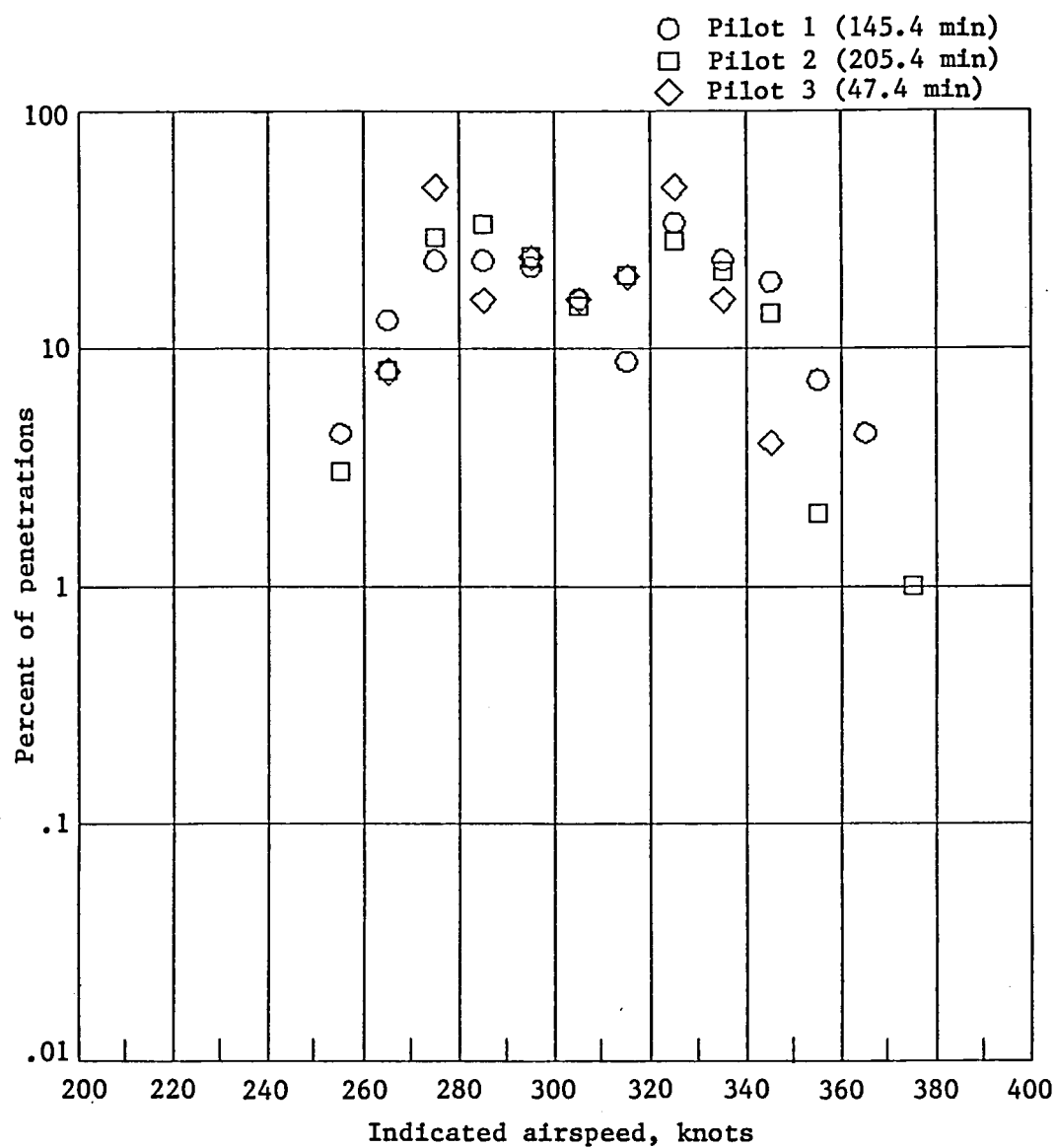
Figure 11.- Continued.

All pilots (398.1 min)



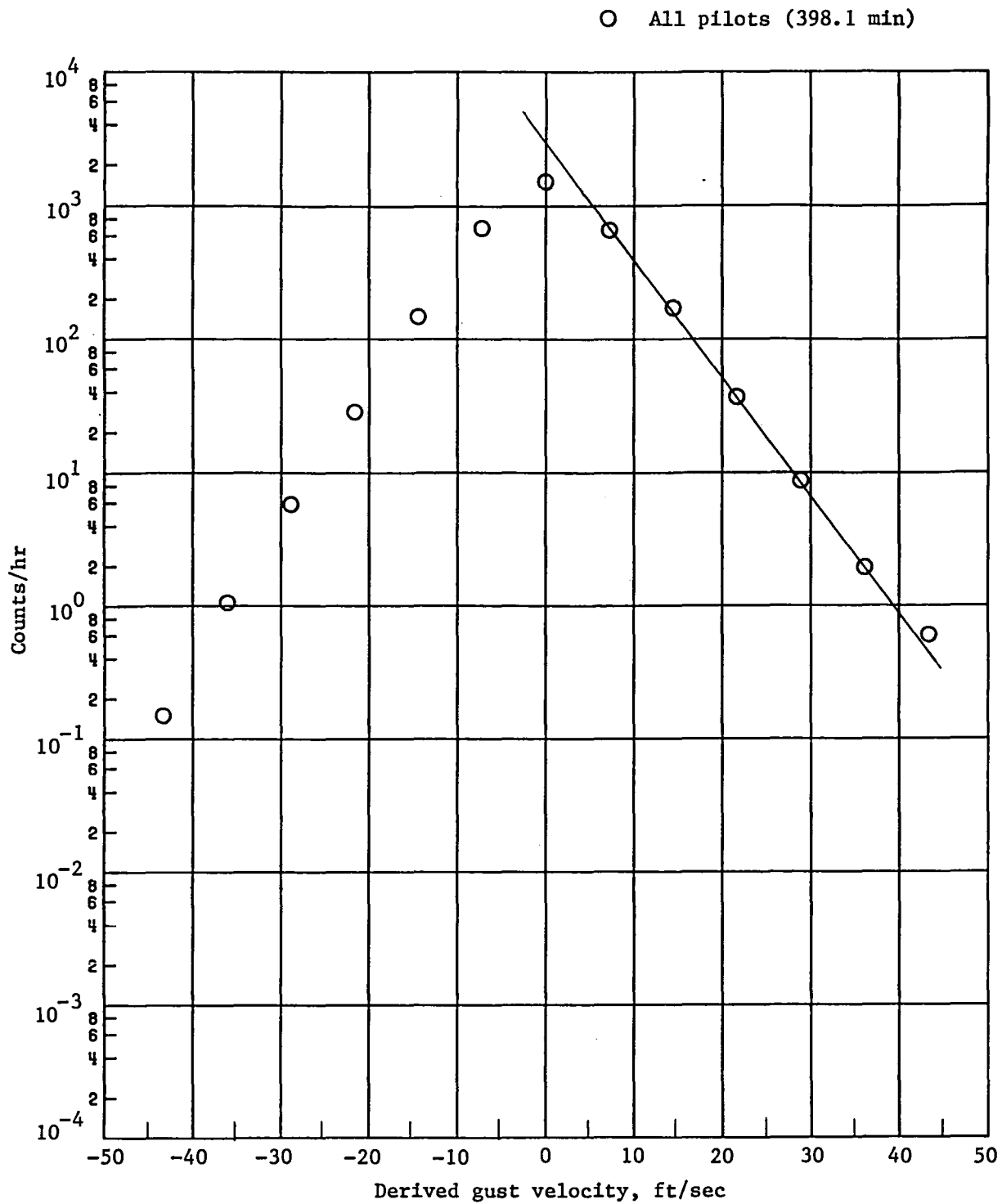
(c) Peak positive and negative occurrences per storm penetration for all data.

Figure 11.- Continued.



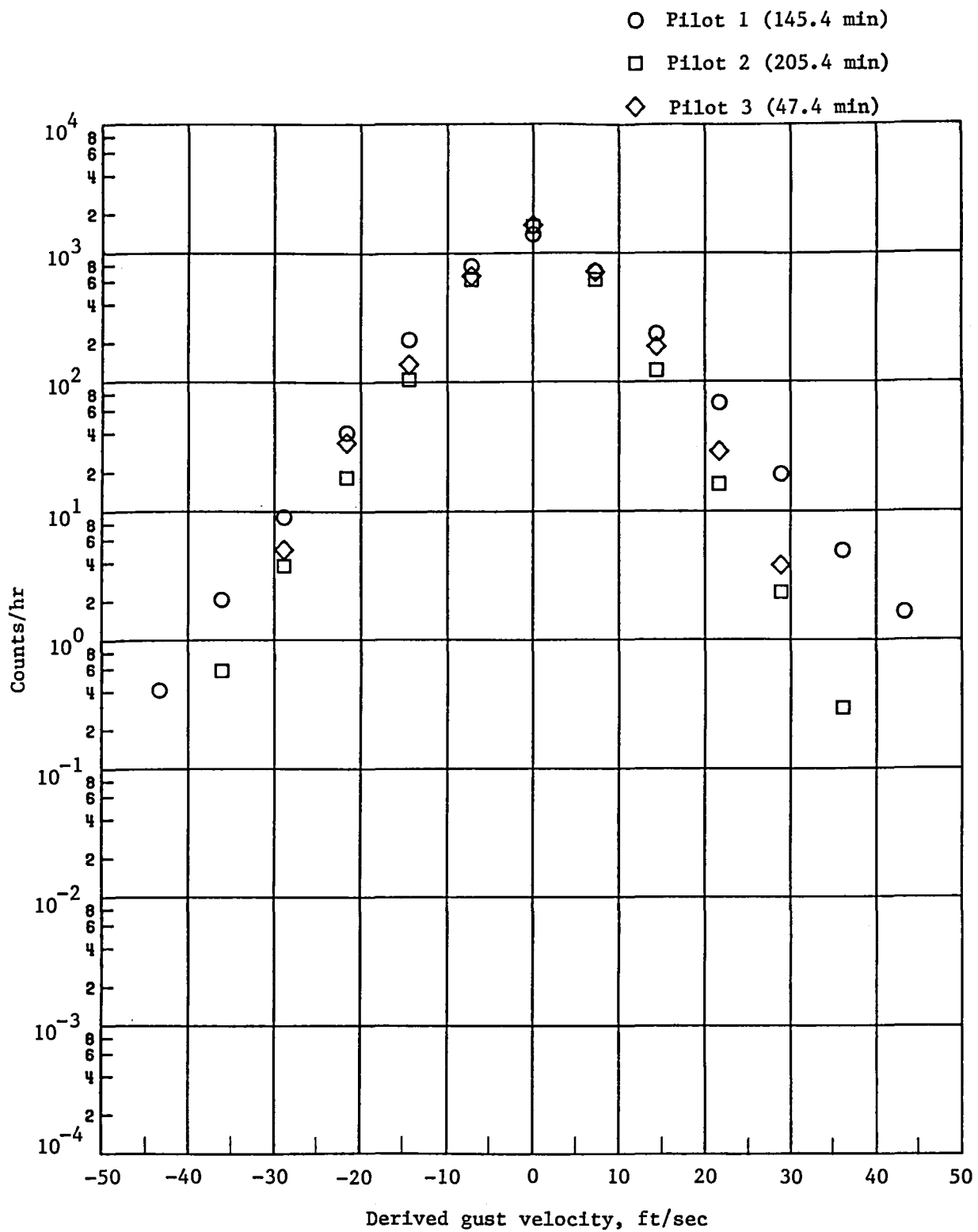
(d) Peak positive and negative occurrences per storm penetration for each pilot.

Figure 11.- Concluded.



(a) Level crossing rates for all data.

Figure 12.- Derived gust velocities from the F-106B while flying inside thunderstorms.

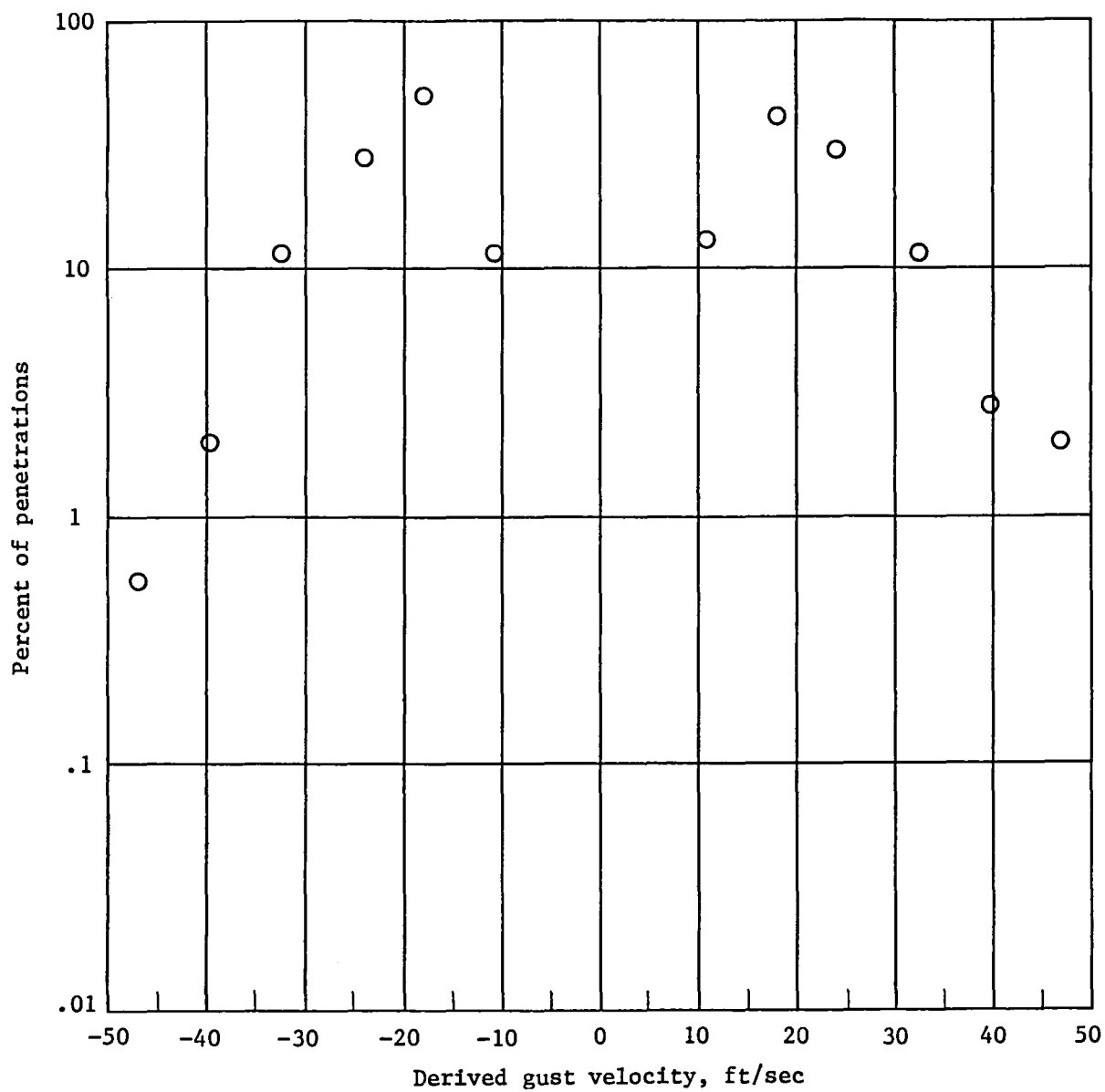


(b) Level crossing rates for each pilot.

Figure 12.- Continued.

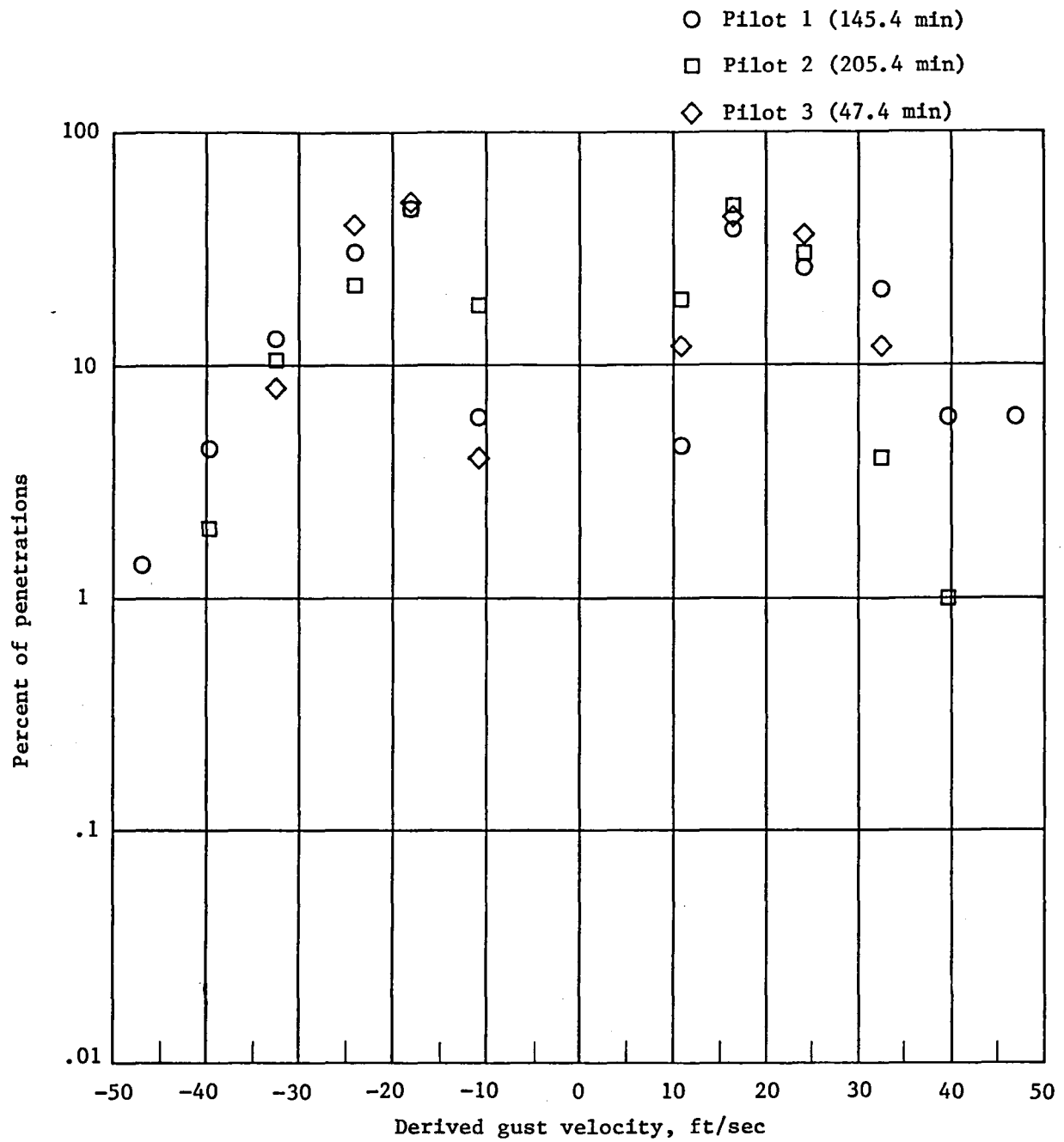


All pilots (398.1 min)



(c) Peak positive and negative occurrences per storm penetration for all data.

Figure 12.- Continued.



(d) Peak positive and negative occurrences per storm penetration for each pilot.

Figure 12.- Concluded.

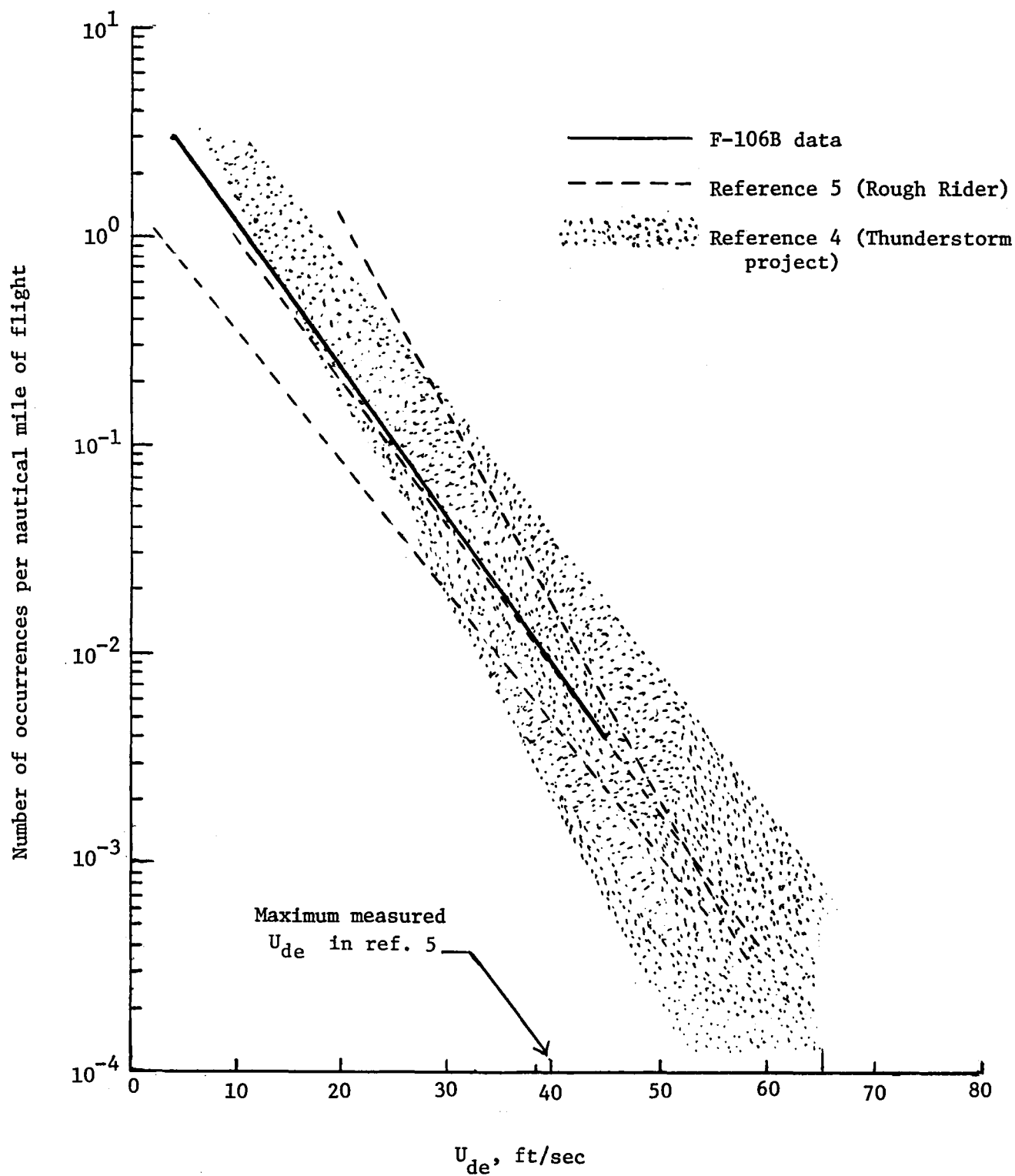


Figure 13.- Comparisons of frequency of turbulence encounters between three programs.

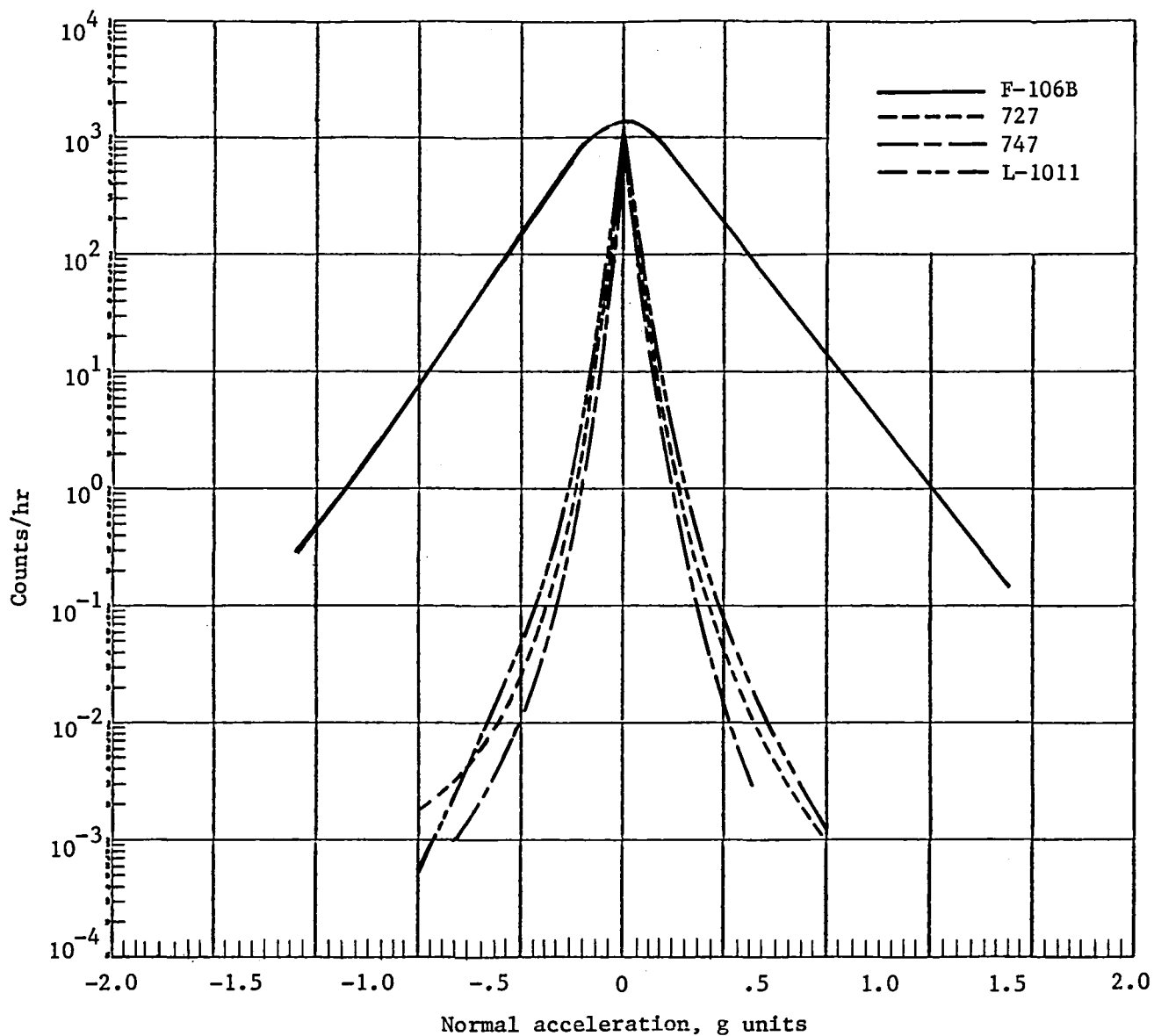


Figure 14.- Comparison of normal acceleration level crossing rates for the F-106B while flying inside thunderstorms with three air transports in normal service.

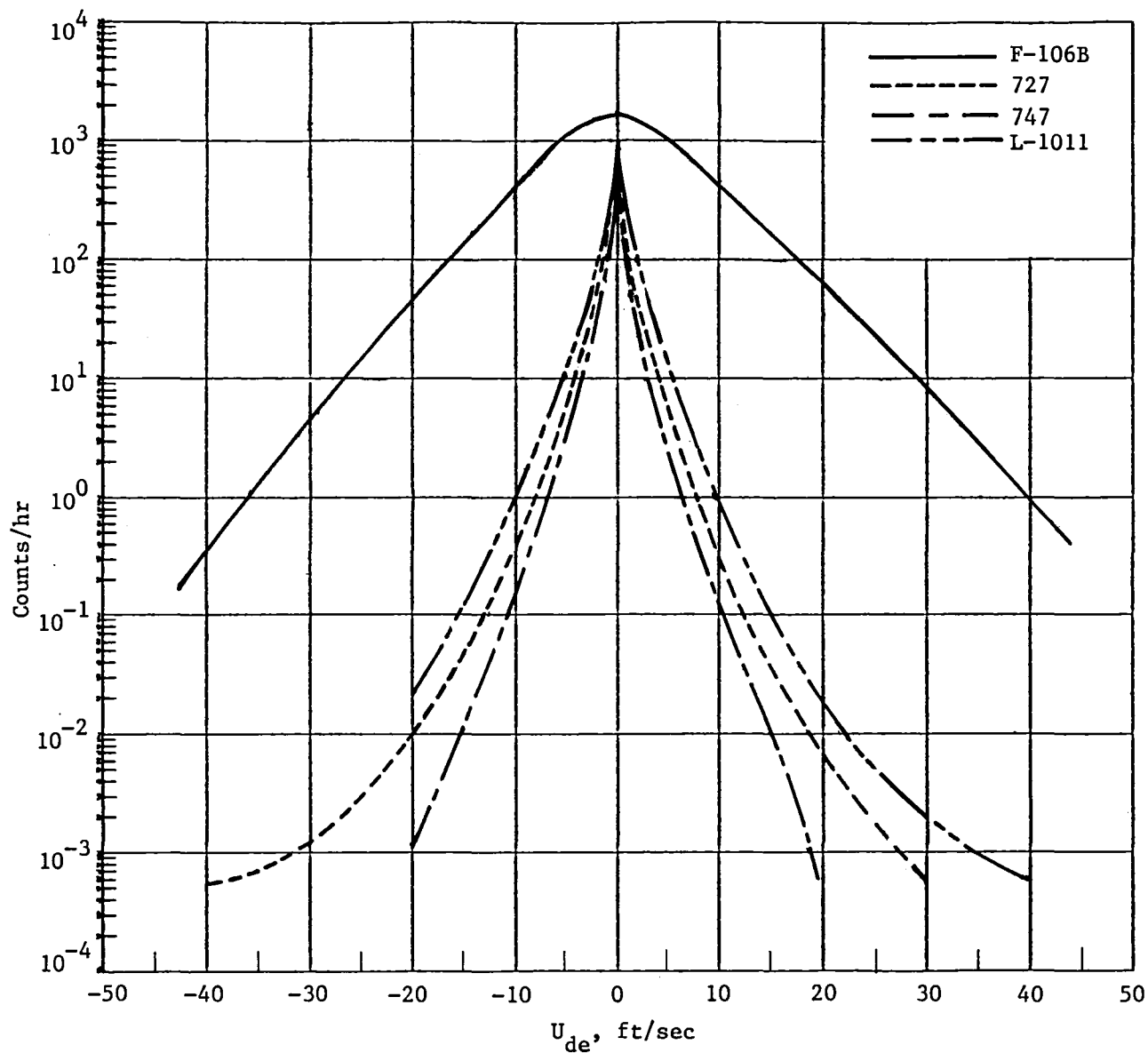


Figure 15.- Comparison of derived gust velocity level crossing rates for the F-106B while flying inside thunderstorms with three air transports in normal service.

**End of Document**